

We are IntechOpen, the world's leading publisher of Open Access books Built by scientists, for scientists

6,900

Open access books available

186,000

International authors and editors

200M

Downloads

Our authors are among the

154

Countries delivered to

TOP 1%

most cited scientists

12.2%

Contributors from top 500 universities



WEB OF SCIENCE™

Selection of our books indexed in the Book Citation Index
in Web of Science™ Core Collection (BKCI)

Interested in publishing with us?
Contact book.department@intechopen.com

Numbers displayed above are based on latest data collected.
For more information visit www.intechopen.com



Auto-Reparation of Polyimide Film Coatings for Aerospace Applications Challenges & Perspectives

A.A. Périchaud, R.M. Iskakov, Andrey Kurbatov, T. Z. Akhmetov, O.Y. Prokohdko, Irina V. Razumovskaya, Sergey L. Bazhenov, P.Y. Apel, V. Yu. Voytekunas and M.J.M. Abadie

Additional information is available at the end of the chapter

<http://dx.doi.org/10.5772/46005>

1. Introduction

In the aerospace industry metal parts are substantially replaced by polymer matrix composites presenting many advantages compared with the metal parts they are replacing. However composite damage is very difficult to detect because it often forms a sub-laminate locations, invisible to the naked eye. To overcome these problems, research in the last two decades has led to the development of self healing polymeric materials that mimic some features found in biological systems. The development of self-healing polymeric materials, those that practically imitate self-healing process of wounds is a new and challenging problem for space applications to protect different types of devices made with composite materials and represents a new paradigm in materials design [1]. The pioneer works in auto-reparation of composites were developed by White S. R et al [2-6]. Their originality was to suggest the encapsulation of monomer – dicyclopentadiene and Grubbs catalysor disseminated uniformly into the composites. Under loading cracks are formed and microcapsules open up releasing monomer and initiator which fulfill the cracks by polymerization and crosslinking reactions and allow the composite to retrieve his original structure without losing its initial mechanical properties - Figure 1.

The concept is strongly dependant on the reactivity of the monomers used as well as the initiator systems [7].

A sub-orbital spaceflight (above 100 km) or a low Earth orbit (LEO) impose on the composites the following conditions : absence of oxygen, temperature variable from -120°C (dark side) to +300°C (solar side), UV and heavy ions radiation, low pressure 10^{-4} Pa. For

example, the International Space Station is in a LEO that varies from 320 km (199 miles) to 400 km (249 miles) above the Earth's surface.

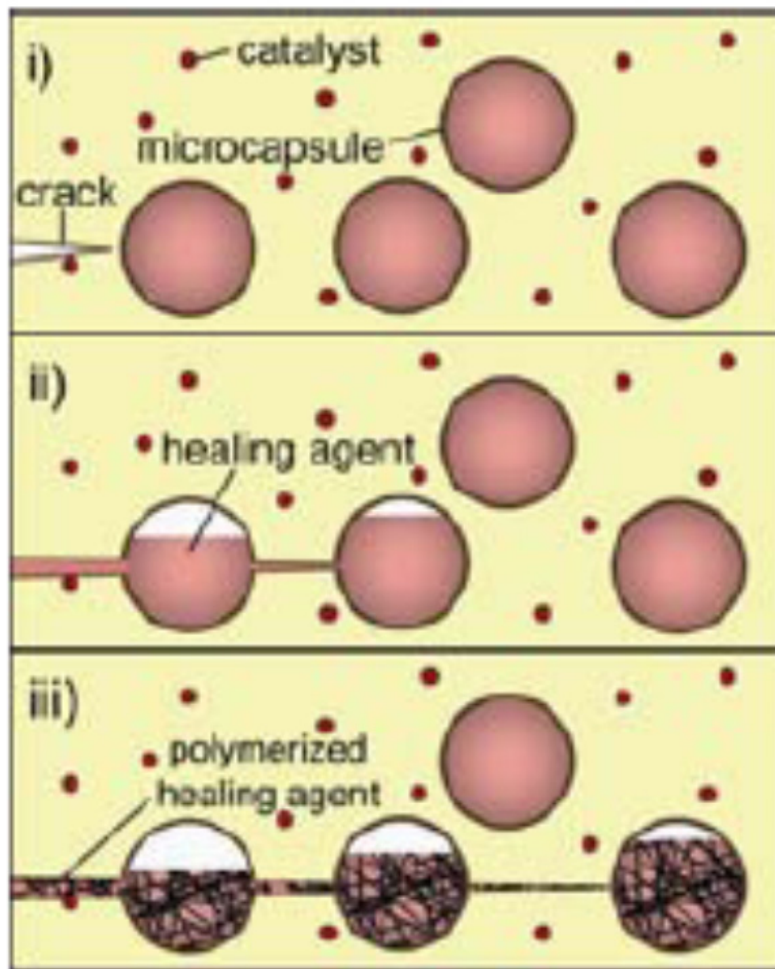


Figure 1. Concept of reservoirs developed by White S. R et al

The methodology developed was to test the feasibility of self-healing by using an encapsulated multifunctional acrylates, i.e. trimethylol propane triacrylate (TMPTA) in presence of a radical photoinitiator (Darocur® 1173).

The novelty of the work was to develop new polymeric film composites, based on Polyimide containing in the same reservoir microencapsulated active monomer and generator of active species, to prevent destruction of the damaged sample.

The new concept tested was to crosslink the monomer in presence of a radical photoinitiator which, upon exposure to UV, produces active centres, permitting the self-healing of the damaged composites.[8]. A schematic of our system is briefly described in Figure 2.

Three major problems have been studied:

1. Develop a suitable microcapsule which could, under loading, liberate the active principle in presence of initiator.

2. Distribute homogeneously the microcapsules into the polymeric film used as coatings
3. Test the new super-composite film and its auto-reparation once micro cracks have been formed, to prevent crack growth and macro damage of the composite.

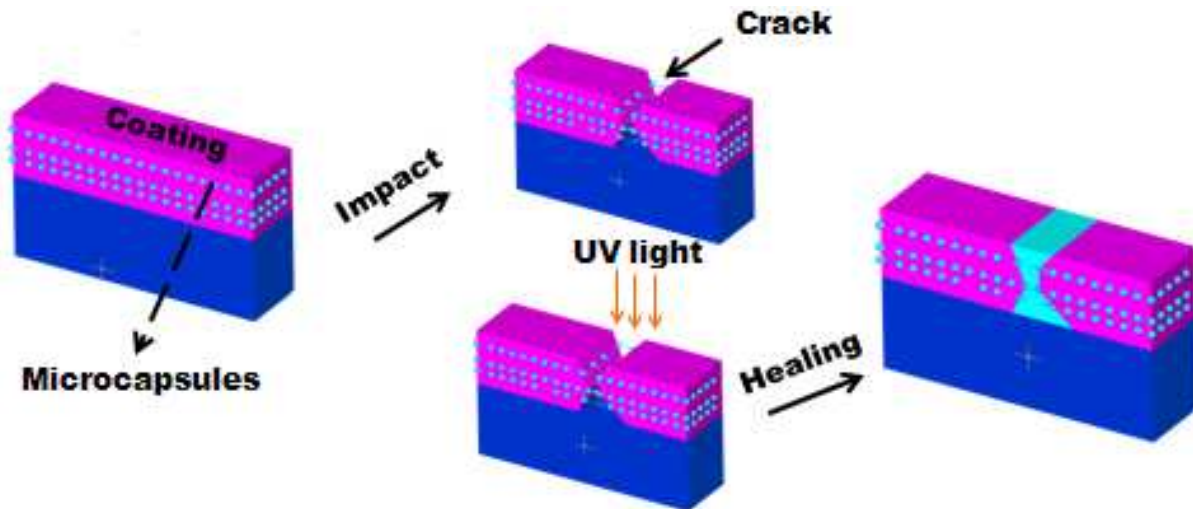


Figure 2. Self-healing of film coatings

2. Microencapsulation

Microcapsules shell should be resistant to high temperatures ($> 300\text{ }^{\circ}\text{C}$) and have average diameters ranging 1-20 μm in order to put them in the host material.

Different models of microcapsules have been tested: Poly(urea/formaldehyde), Polyurethane and Silica gel

2.1. Synthesis of poly(urea-formaldehyde) microcapsules

The healing agent (trimethylol propane triacrylate TMPTA monomer) and the photoinitiator (Darocur[®] 1173) presented in – Figure 3, are encapsulated in poly(urea-formaldehyde) by *in situ* polymerization – Figure 4.

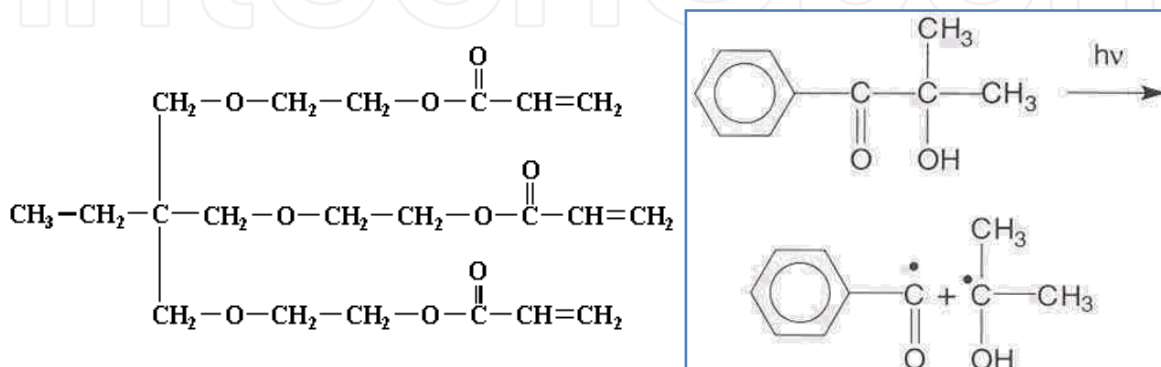


Figure 3. TMPTA monomer and Darocur[®] 1173 photoinitiator

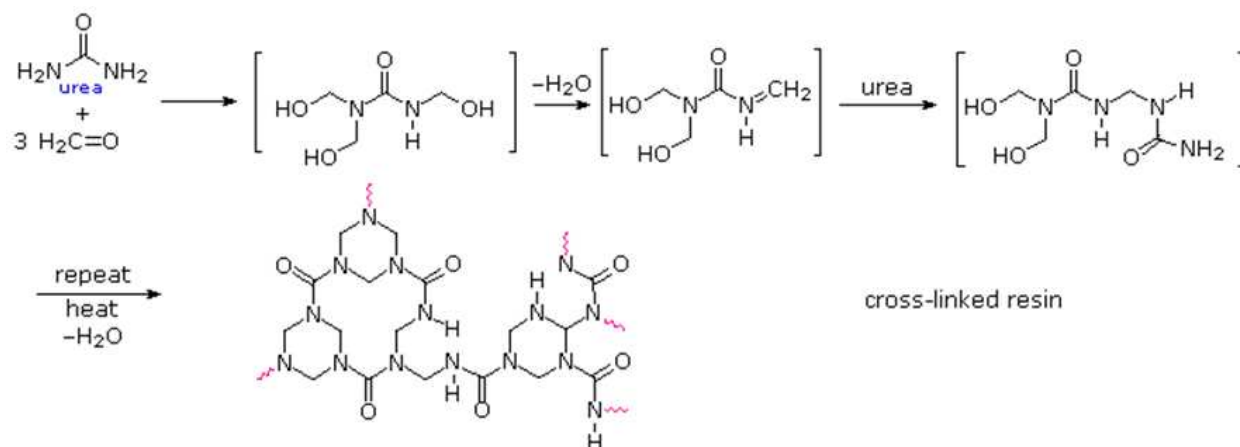


Figure 4. Poly(urea-formaldehyde) resin

These microcapsules are carried out by *in situ* polymerization in direct emulsion (Oil/Water). At room temperature, deionized water and aqueous solution of ethylene maleic anhydride (EMA) are mixed in a reactor. The reactor is placed in a temperature-controlled oil bath on a programmable hot plate with external temperature probe and the solution is agitated with a mechanical stirrer. Under agitation, urea, ammonium chloride and resorcinol were dissolved in the solution. The pH is raised from ~ 2.6 to 3.5 by drop-wise addition of sodium hydroxide (NaOH) and hydrochloric acid (HCl). One or two drops of 1-octanol are added to eliminate surface bubbles. Then, the healing agent (TMPTA monomer) and the photoinitiator (Darocur[®] 1173) are added slowly in the solution to lead to a stable emulsion. After 10 minutes of stabilization, an aqueous solution of formaldehyde (37 wt. %) is incorporated in the emulsion to obtain 1:1:9 molar ratio of formaldehyde to urea. The emulsion is covered and heated at 55°C for 5 hours. After 5 hours of continuous agitation, the mixer and hot plate are switched off. Once cooled to ambient temperature, particles are filtered on Büchner and are washed with a water/ethanol solution (50 wt. %/50 wt. %). Then, particles are dried in air at room temperature for 24-48 h – Figure 5.

Scanning Electron Microscopy - The morphology of particles (surface and form) is investigated by Environmental Scanning Electron Microscopy (ESEM). The particles are spherical with average diameter in the range of 2-30 μm – Figures 6 (a) & 6 (b). The shell of microparticles presents two type of surface: one has a smooth surface – 6 (a), or a rough surface – Figure 6 (b). The Figure 6 (c) illustrates a poly(urea-formaldehyde) microcapsule which has been ruptured under physical constraint (pressure).

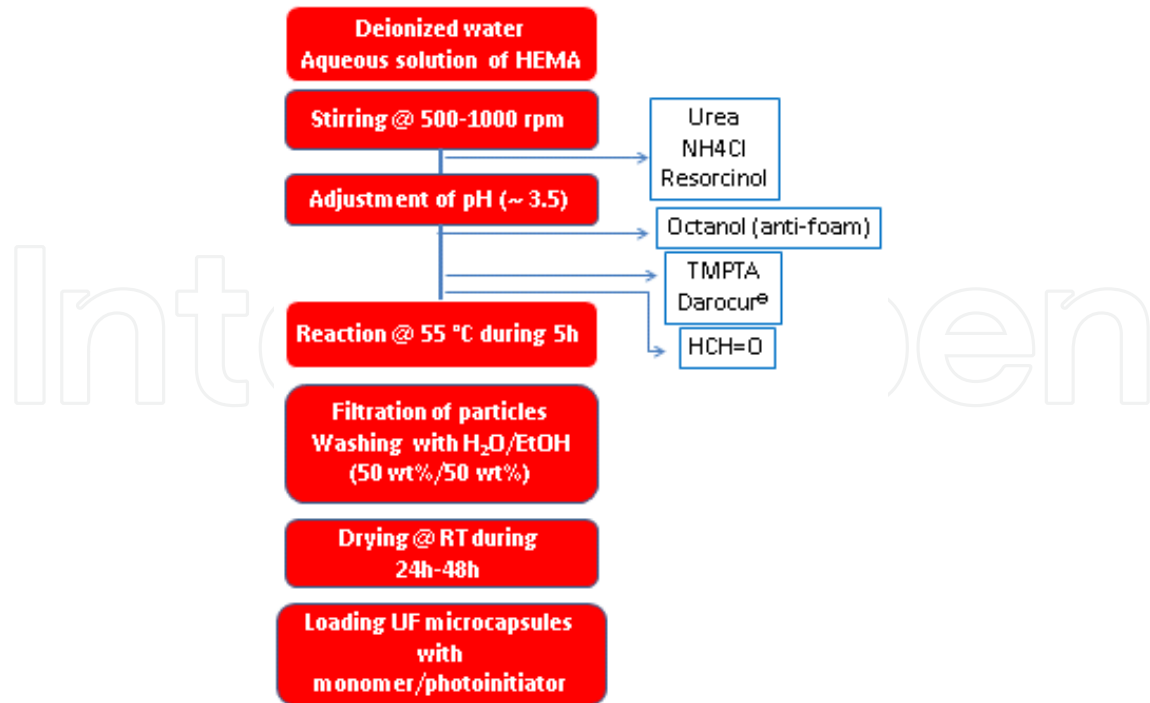


Figure 5. Schematic of the encapsulation process with poly(urea-formaldehyde)

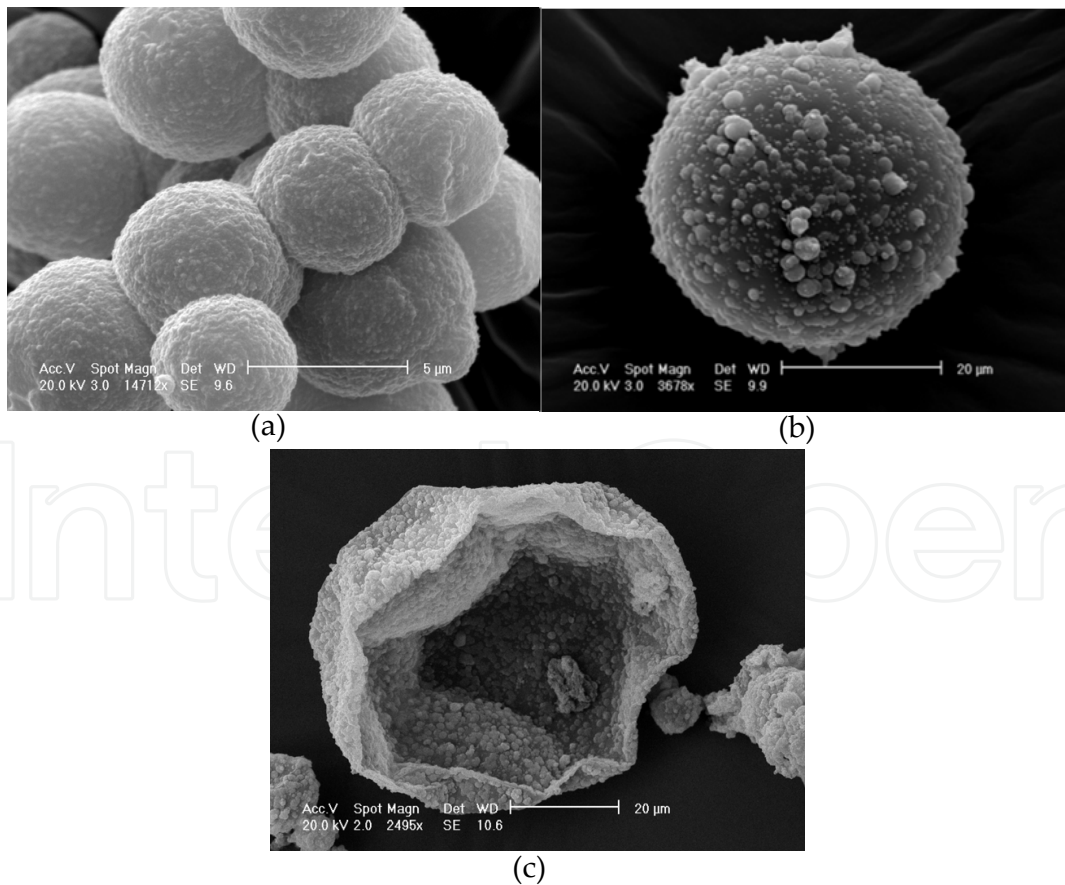


Figure 6. ESEM image of (a) UF microcapsules loading in TMPTA monomer and Darocur[®] 1173 photoinitiator with a smooth surface, (b) UF microcapsules loading in TMPTA monomer and Darocur[®] 1173 photoinitiator with a rough surface and (c) ESEM image of ruptured Urea-Formaldehyde microcapsule

Infrared Analysis - The comparison between infrared spectra of UF empty microparticles – Figure 7 (a) and UF microparticles loaded in TMPTA – Figure 3 (b), shows the presence of new bands, in particular at 1722 cm^{-1} (C=O stretching vibration), 983 cm^{-1} (wagging of the =CH₂ group), and 808 cm^{-1} (twisting of the =CH₂ group), characteristic bands of TMPTA which indicates that this compound has been encapsulated in UF microcapsules.

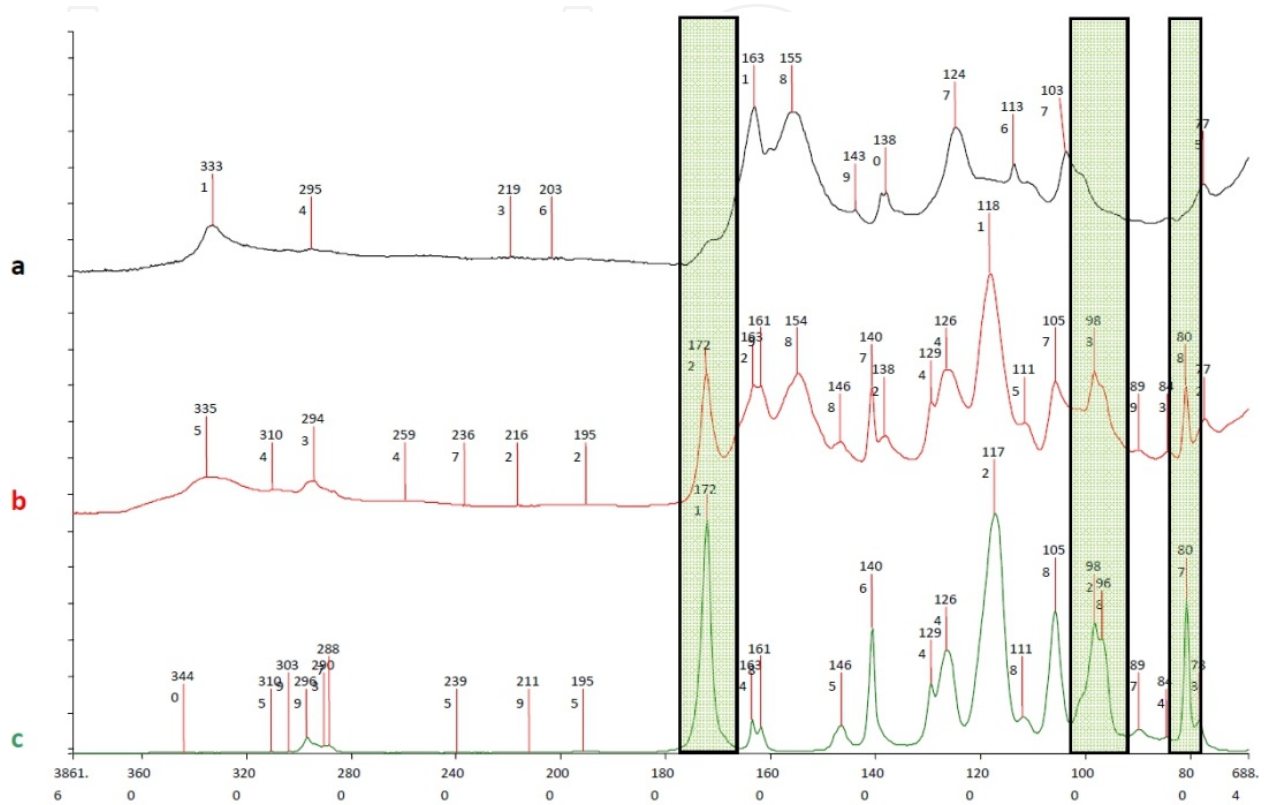


Figure 7. Infrared spectrum of (a) Empty UF microcapsules, (b) broken UF microcapsules loaded with TMPTA and (c) TMPTA monomer

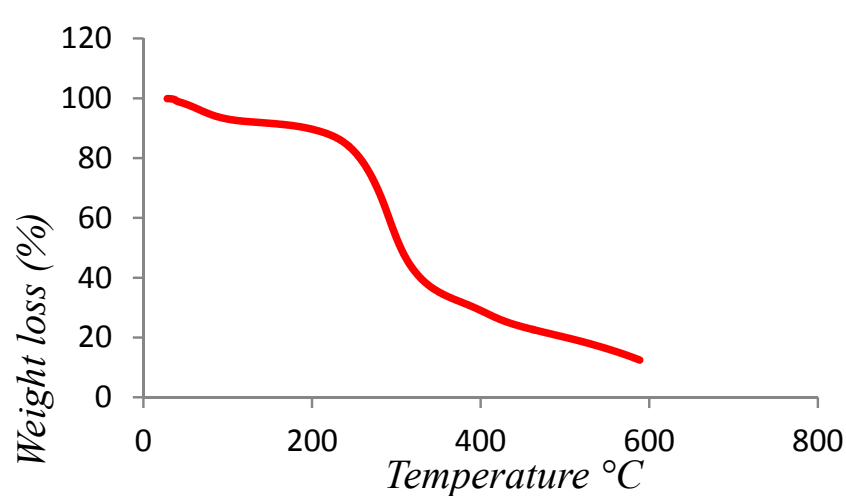


Figure 8. TGA of empty UF microcapsules

Thermogravimetric Analysis - Empty UF microcapsule shows – Figure 8, a weight loss (around 10 %) until 110 °C corresponding to the evaporation of free water in microcapsules, and an important decreasing in weight (around 80 %) starting from 180 °C due to the decomposition of urea-formaldehyde microparticles. Therefore the urea formaldehyde could not be used to self-heal spatial device composites because of polymer decomposition below 300 °C (maximum temperature in space).

2.2. Synthesis of poly(urethane) microcapsules by interfacial polycondensation

The TMPTA monomer and the Darocur® 1173 photoinitiator are encapsulated in polyurethane microcapsules by *in situ* polymerization. Microcapsules are obtained by *in situ* polymerization in direct emulsion (Oil/Water). At room temperature, deionized water and polyvinyl alcohol PVOH (3 wt. %) are mixed in a reactor equipped with a mechanical stirrer. Then, an organic solution of monomer (Hexamethylene diisocyanate HMDI/chloroform) containing the monomer (TMPTA) and photoinitiator (Darocur® 1173) to be encapsulated is added to the aqueous solution leading to a stable Oil/Water emulsion. After 5 minutes of stabilization, a hydrophilic monomer (Ethylene Diamine EDA in excess) is added to the emulsion – Figure 9. The reaction is continued until stabilization of the pH (around 5 hours).

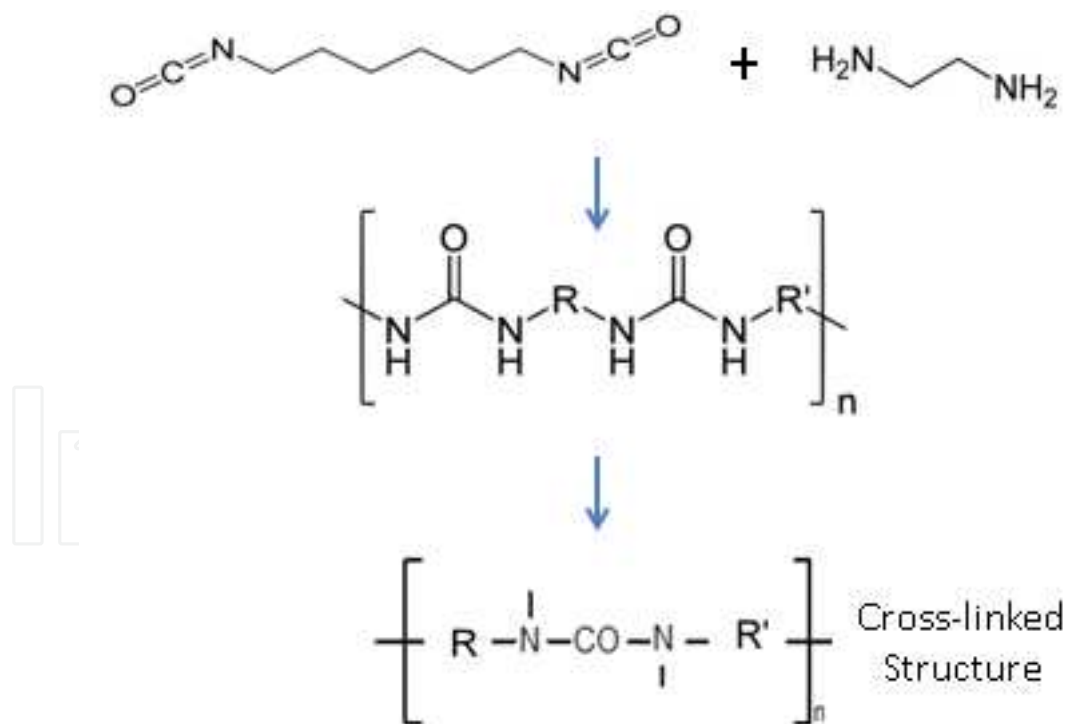


Figure 9. Cross-linked structure of polyurethane with R = $-(\text{CH}_2)_6-$ and R' = $-(\text{CH}_2)_2-$

Then, particles are separated under vacuum with a Büchner system and are rinsed with an ethanol/deionized water mixture (50 wt. %/50 wt. %). Microparticles are collected and are air dried during 24-48 h – Figure 10.

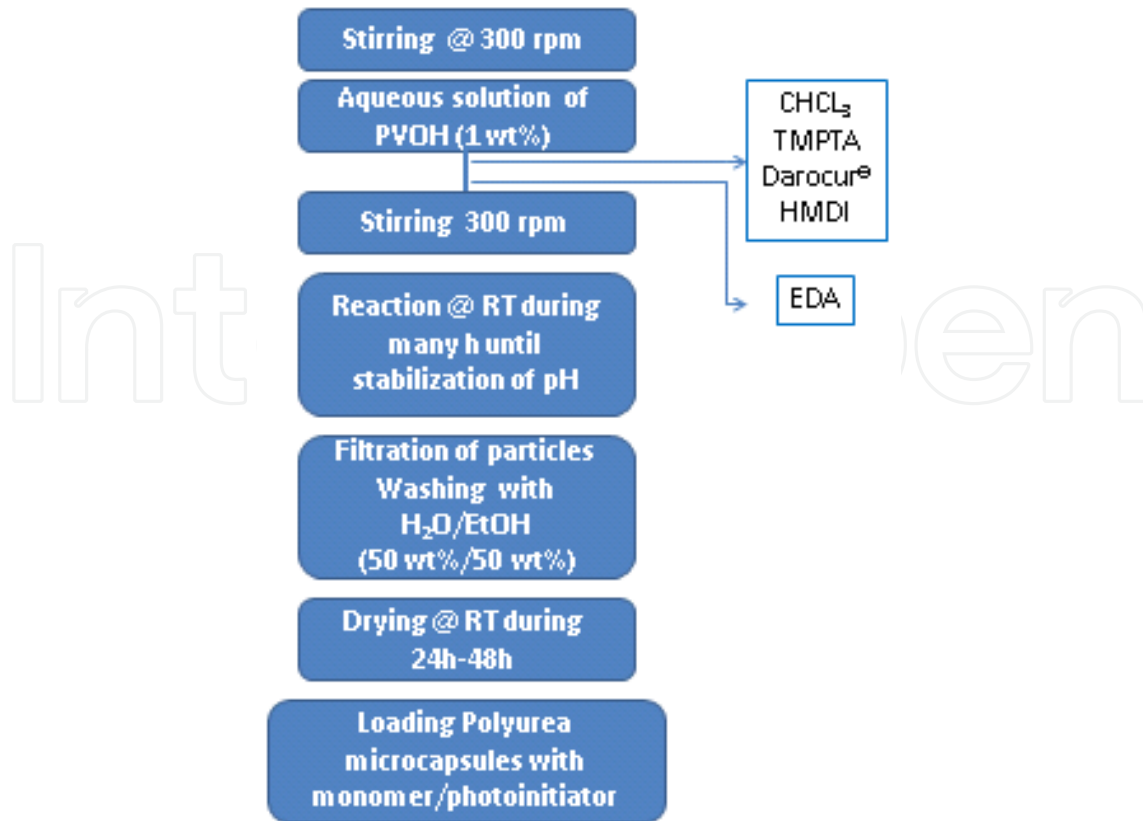


Figure 10. Schematic of the encapsulation process with polyurethane

Scanning electron microscopy - Particles were examined by ESEM. The particles are spherical with average diameter in the range of 200-300 μm and the membrane of microparticles is smooth, as shown in – Figure 11.

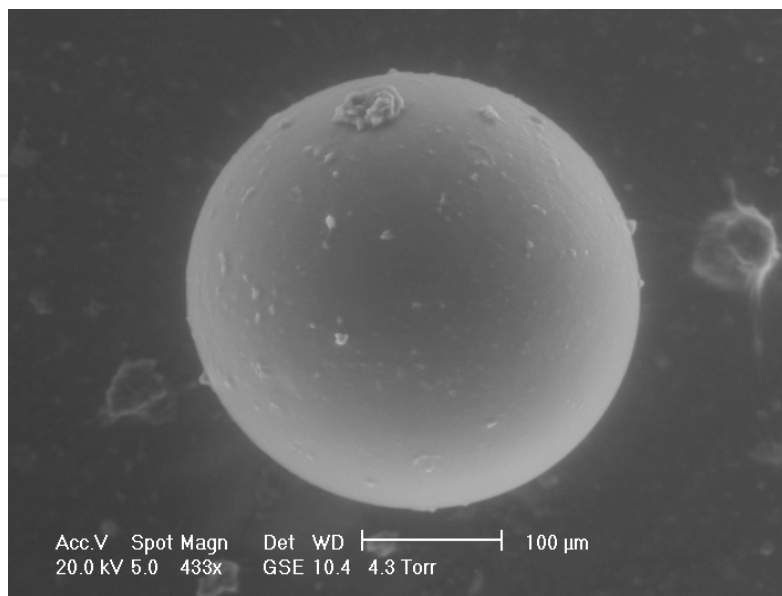


Figure 11. ESEM image of Poly(urethane) microcapsules loaded with TMPTA monomer and Darocur[®] 1173 photoinitiator

Infrared Analysis - The comparison between Infrared spectrums of the empty polyurethane microparticles - Figure 12 (b), and polyurethane microparticles loaded in TMPTA – Figure 12(c) shows the presence of new bands, in particular at 1721 and 983 cm^{-1} and confirm that TMPTA monomer has been encapsulated in polyurethane microcapsules.

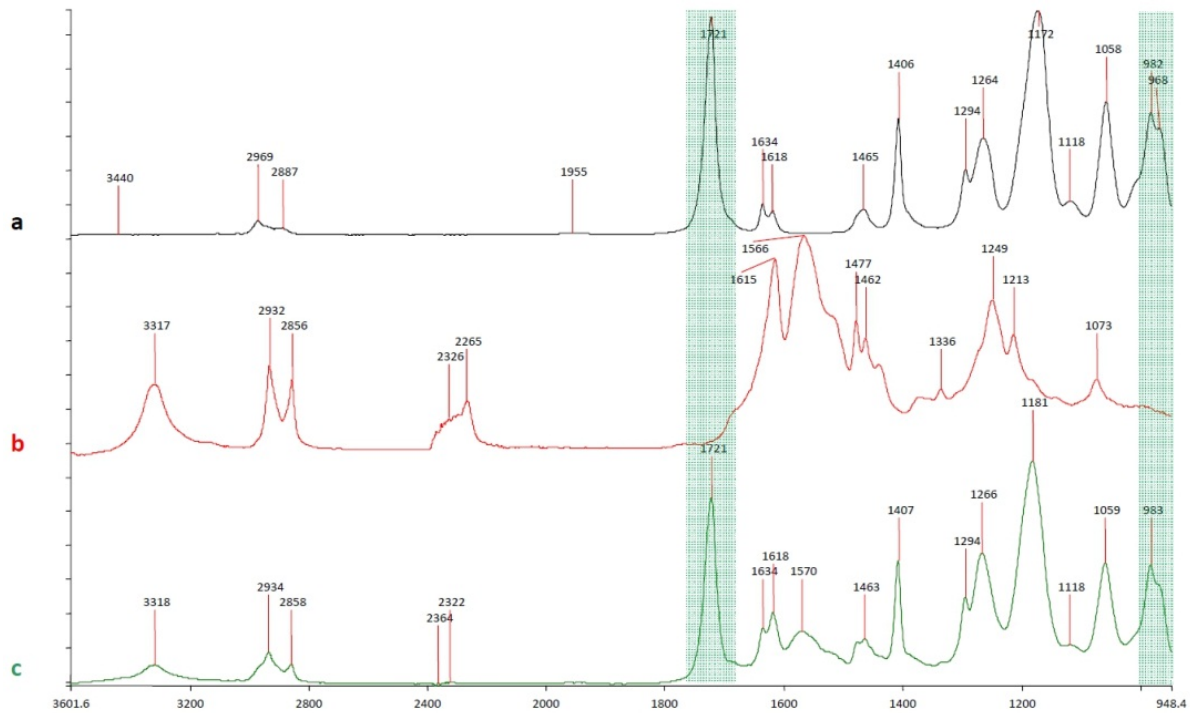


Figure 12. Infrared spectrum of (a) TMPTA, (b) empty polyurethane microparticles and (c) polyurethane microcapsules loaded with TMPTA monomer

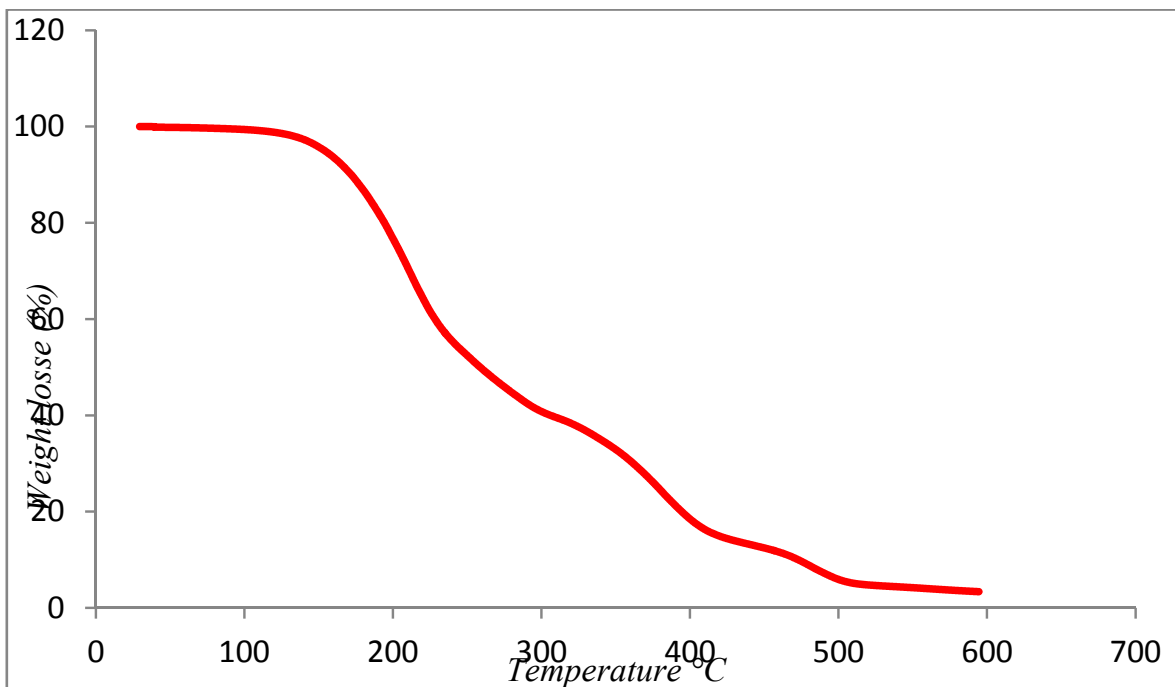


Figure 13. TGA of empty polyurethane microcapsules

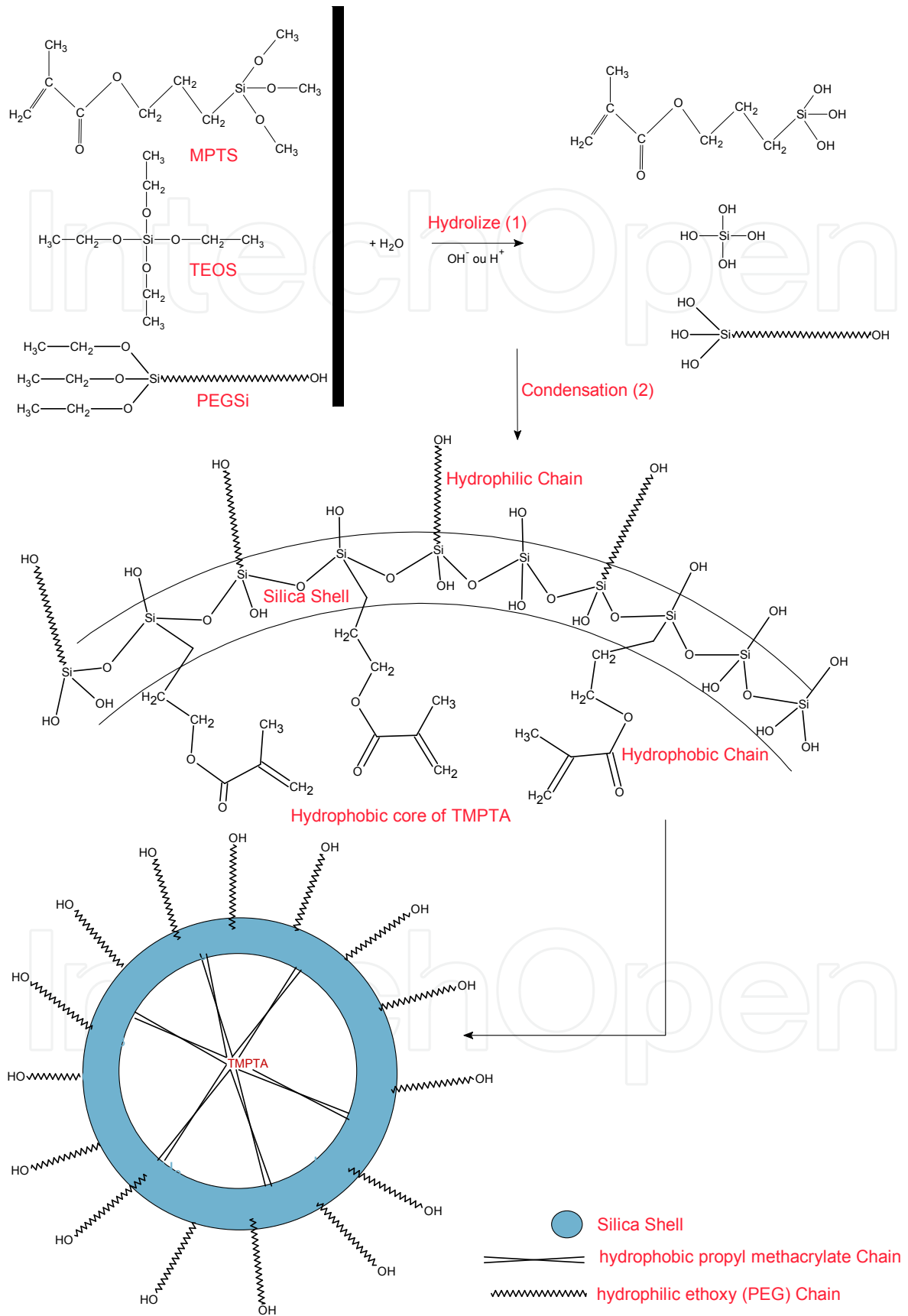


Figure 14. Schematic Road for Synthesis of Silica-Gel Microcapsules Loaded with TMPTA

Thermogravimetric Analysis - The thermogravimetric analysis of polyurethane microcapsules (without monomer) – Figure 13, presents a decreasing in weight (above 200°C) due to the deterioration of polymer. Therefore, this polymer is not a good candidate as well to encapsulate healed agent for aerospace applications.

2.3. Synthesis of silica-gel microcapsules by sol-gel polymerization process

The TMPTA monomer and the Darocur® 1173 photoinitiator are encapsulated in silica gels microcapsules by sol-gel polymerization. 3-(trimethoxysilyl)propyl methacrylate (MPTS), tetraethoxysilane (TEOS), trimethylol propane triacrylate (TMPTA), Darocur® 1173, silica surfactant PEGSi (compatibility agent to increase the stability between the shell and the aqueous solution) and ethanol are mixed with a magnetic stirrer in a bottle. Then, an aqueous solution of ammoniac (16 wt. %) is added drop by drop to the mixture. After 10 minutes of continuous agitation, this solution is added to an aqueous solution of polyoxyethylene 1,2- nonylphenyl ether (Igepal CO-720 (NP12) at 1 wt. %. After 2 hours of reaction, the suspension is filtered under vacuum. Microparticles are collected and are dried in air at room temperature for 24-48 h. Figure 14 illustrates the schematic road to synthesis of silica-gel microcapsules loaded with TMPTA monomer [9].

Scanning Electron Microscopy - Silica microcapsules are studied by ESEM. The spherical particles have average diameters ranging from 1-30 μm , shown in - Figure 15. The shells of microparticles present a smooth surface.

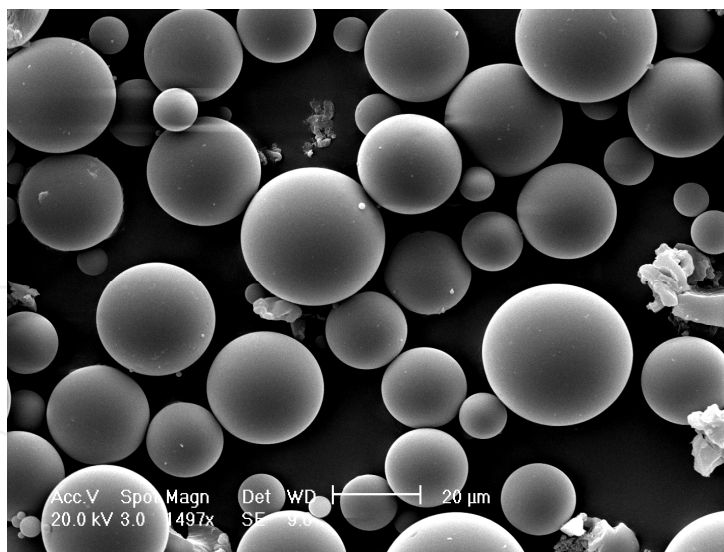


Figure 15. ESEM image of Silica-gel microcapsules loading with TMPTA monomer and Darocur® 1173 photoinitiator

Infrared Analysis - The comparison of IR spectra of empty silica-gel microparticules and silica-gel microparticules loaded with TMPTA do not enable us to prove the encapsulation of the TMPTA. In effect, the two spectra present the same absorption bands because silica-gel shell contains a methacrylate compound – Figure 16.

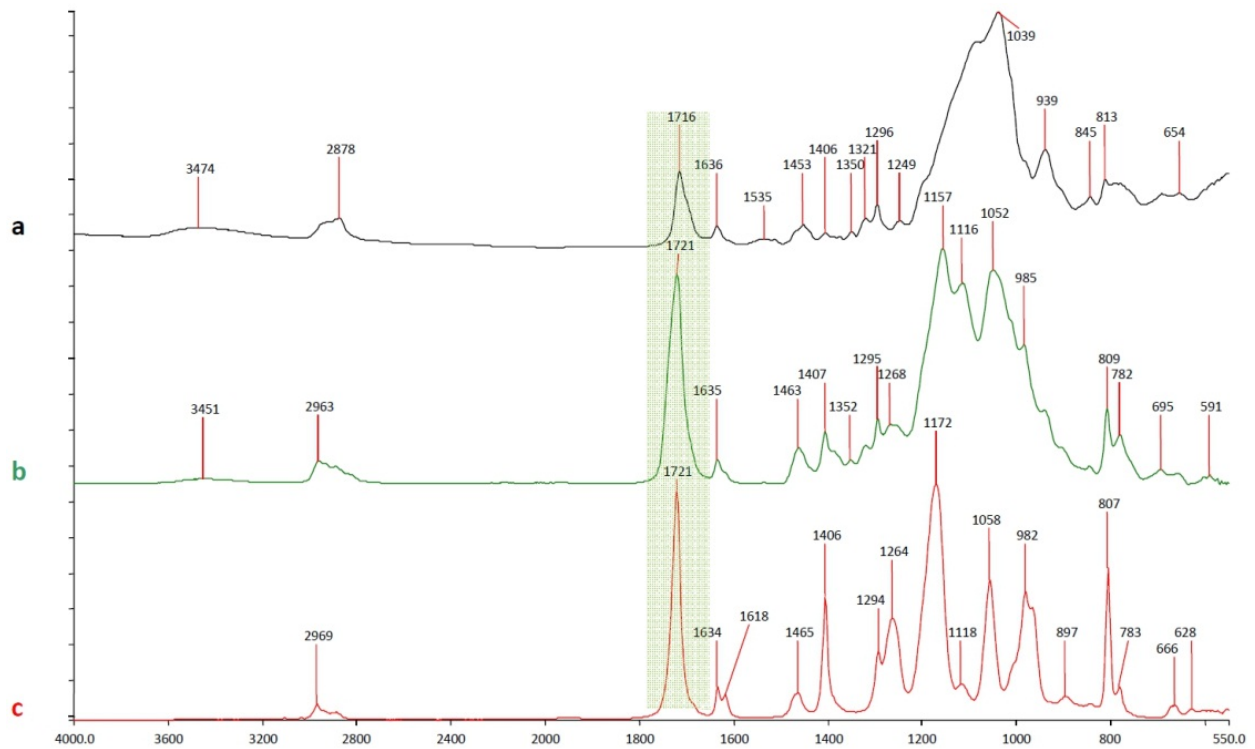


Figure 16. Infrared spectrum of (a) Empty silica-gel microcapsules (b) silica-gel microcapsules loaded with TMPTA monomer and (c) pure TMPTA

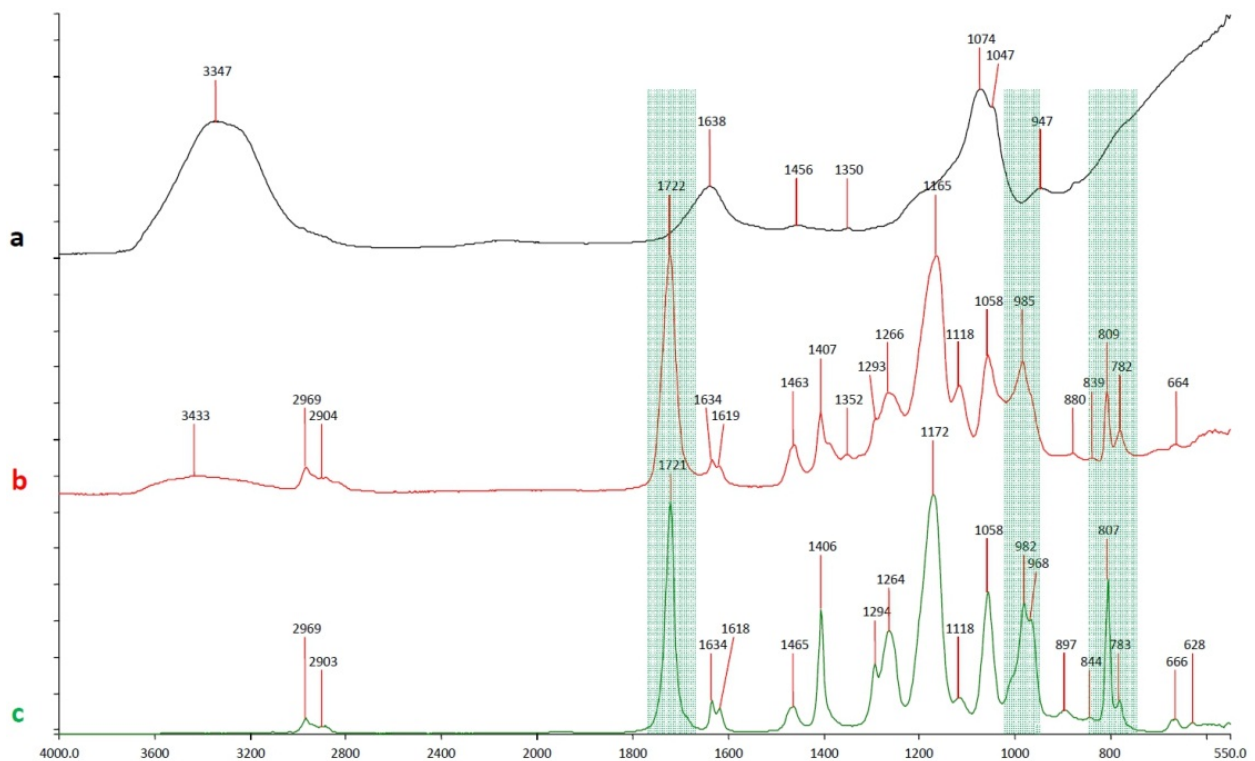


Figure 17. Infrared Spectrum of (a) empty silica-gel microcapsules with TEOS precursor alone, (b) silica-gel microcapsules with TEOS precursor alone loaded with TMPTA monomer and (c) pure TMPTA

For that we have used silica-gel microcapsules (empty microcapsules and microcapsules loaded with TMPTA) with TEOS precursor alone (not methacrylate chain in this compound). The comparison between Infrared spectra of the empty silica-gel microparticles with TEOS precursor alone – Figure 17 (a) and silica-gel microparticles loaded with TMPTA – Figure 17 (c), shows the presence of new bands, in particular at 1721, 983 and 807 cm^{-1} . These bands, characteristic of the TMPTA monomer, confirm the presence of TMPTA encapsulated in silica-gel microcapsules.

Thermogravimetric Analysis - The thermogravimetric analysis of silica-gel particles (without TMPTA) indicates a good thermal resistance (above 320°C) of silica-gel membranes – Figure 18.

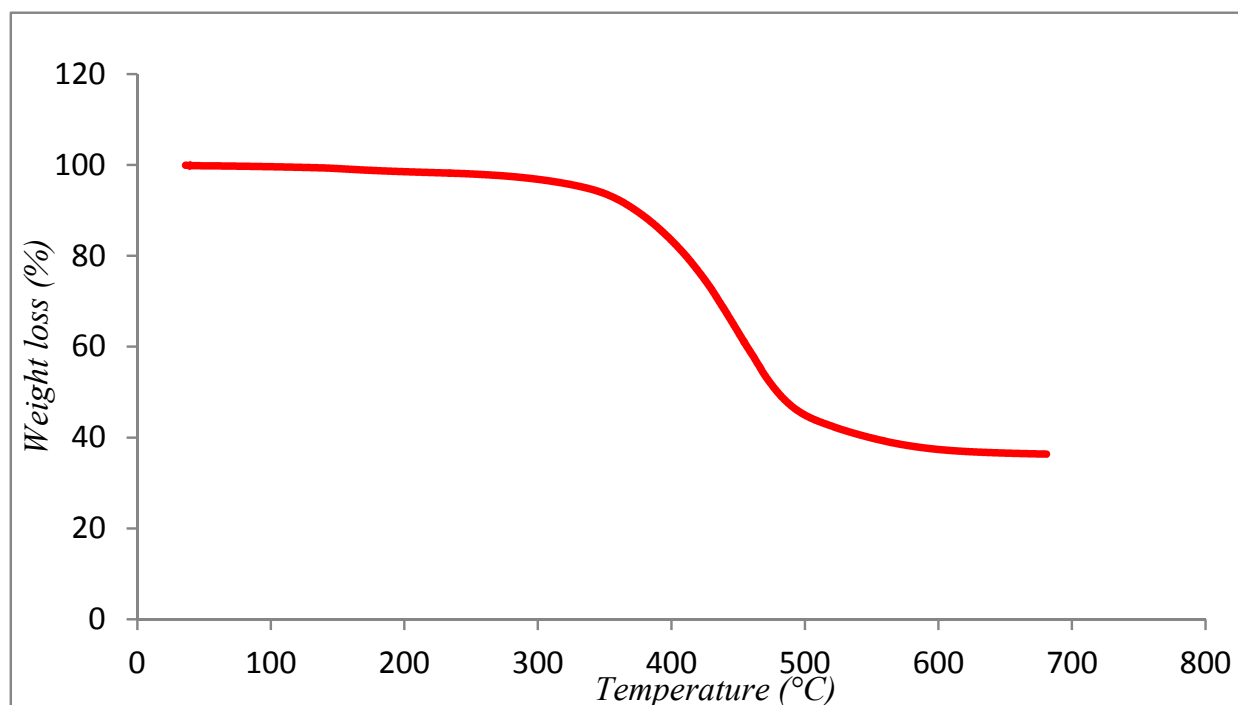


Figure 18. Thermogravimetric Analysis of Empty Silica-gel Microcapsules

We have encapsulated with success TMPTA monomer by different processes of microencapsulation. Two of three techniques used cannot be applicable for aerospace application as the microcapsules are not thermal resistant above 300 °C, presenting a temperature of degradation below 200°C. However, silica membrane is much more resistant due to their degradation temperatures exceeding 300°C.

3. Dispersion into the polyimide film

Polyimide films are based on dianhydride of dicyclodecene tetracarboxylic acid and oxydianiline ODA – Figure 19. The dianhydride was synthesized by Solar-irradiation technology of a mixture of benzene/toluene fraction with maleic anhydride to produce highly reactive monomer – benzene adduct (AB) – Figure 20.

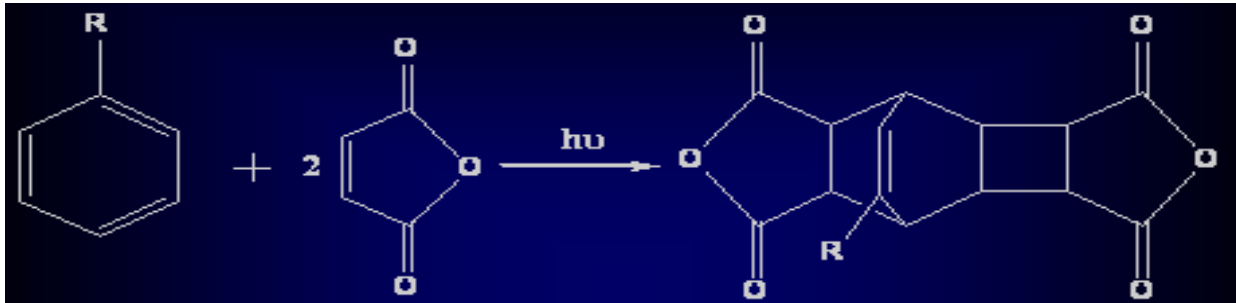


Figure 19. Photosynthesis of the dianhydride of dicyclopentadiene tetracarboxylic acid

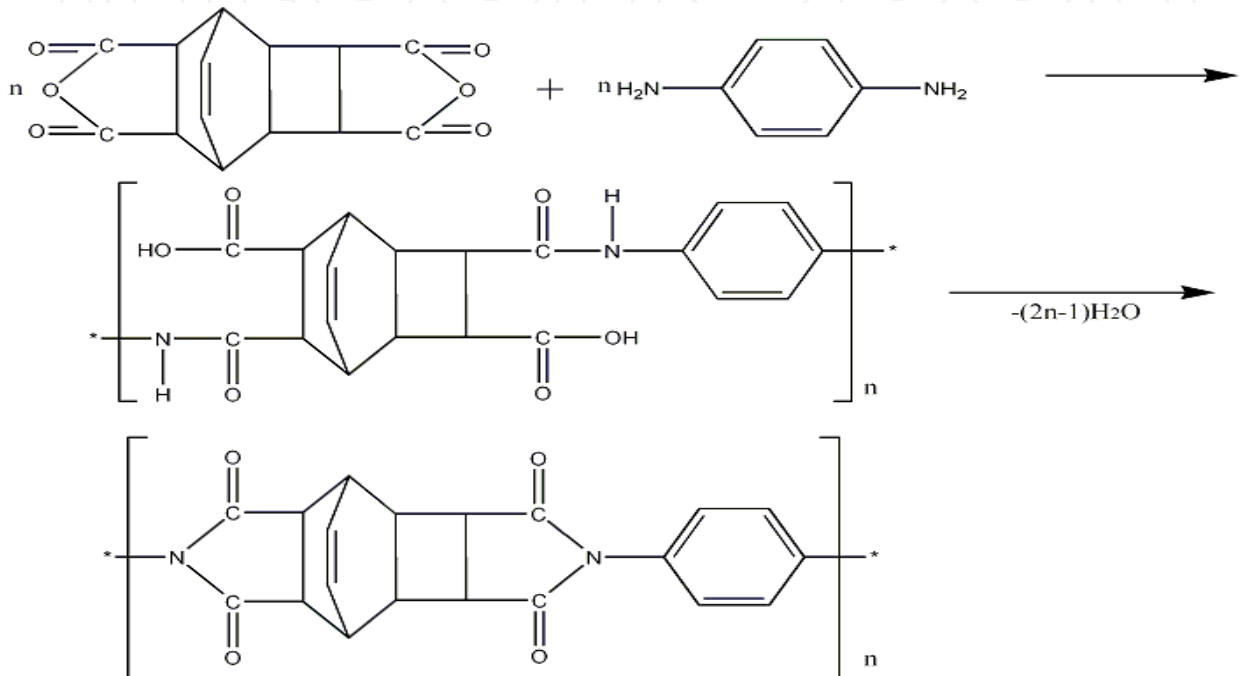


Figure 20. Polyimide based on dianhydride of dicyclopentadiene tetracarboxylic acid and ODA

Microcapsules loaded with TMPTA and the radical photoinitiator are mixed in 5 to 15 wt. % in solution of polyimide in DMF, cast and dry, and then subjected to 100 °C for 4 hours, followed by 4 hours at 180 °C.

Environmental scanning electronic microscopy coupled with RX (ESEM/EXD) – Figure 21(a) and 21(b), show a good dispersion of the microcapsules along the polyimide film and confirm their presence.

EDX of polyimide film does not show any silicium peak - Figure 21 (a) but this peak is present in the analysis of the polyimide with silica-gel microcapsules.

4. Auto-reparation of polyimide film

Different formulation of Polyimide films have been loaded with variable concentration of microcapsules from 5 wt. % to 15 wt. %. Then the films casted are exposed to UV light (365 nm) once cracks were produced – Figures 22 & 23.

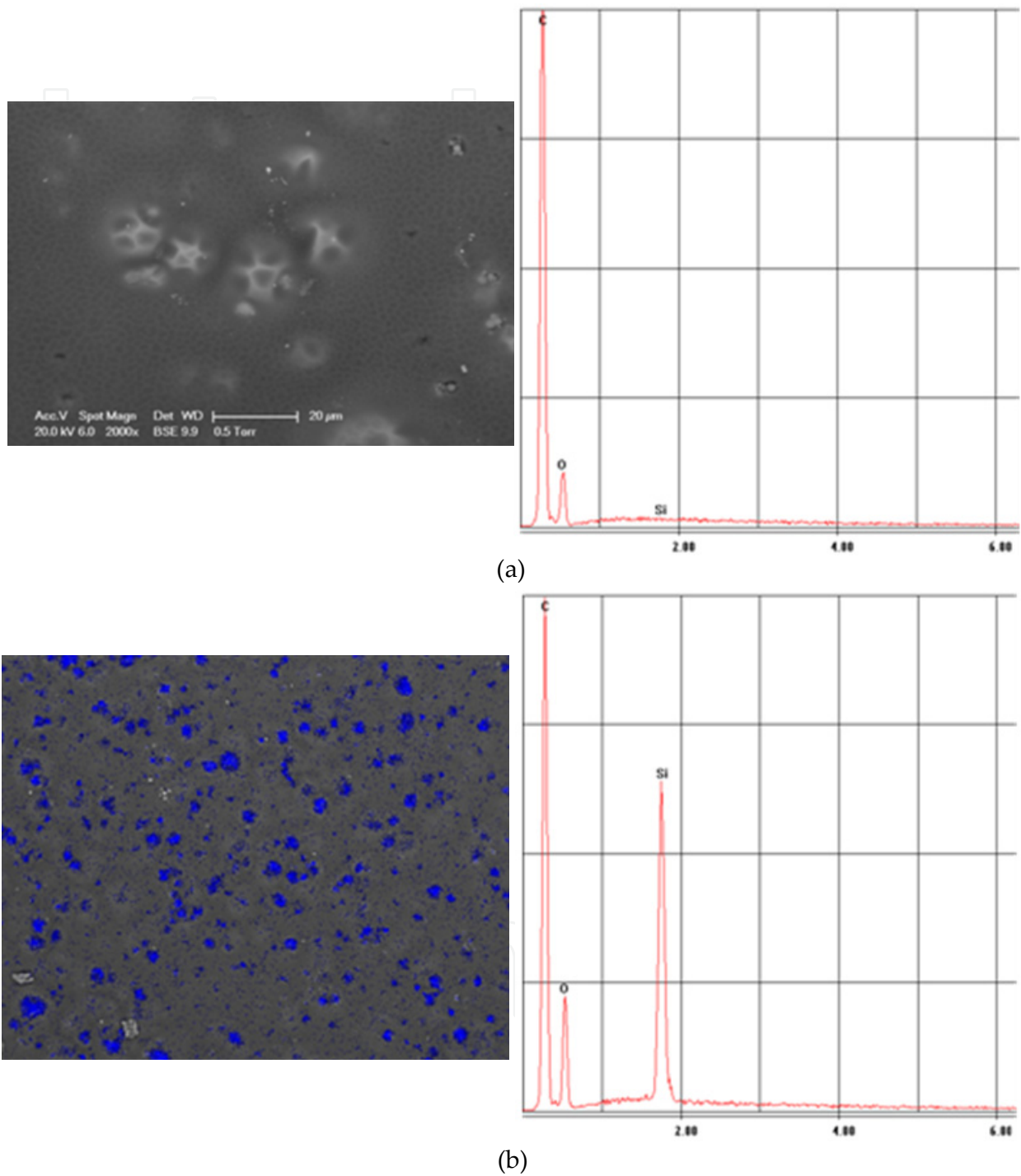


Figure 21. (a) Surface aspect of the polyimide film without microcapsules & EDX
 (b) Surface aspect of the polyimide film with microcapsules & EDX

Self-healing process was followed by morphological analysis shown by environmental scanning electron microscopy ESEM.

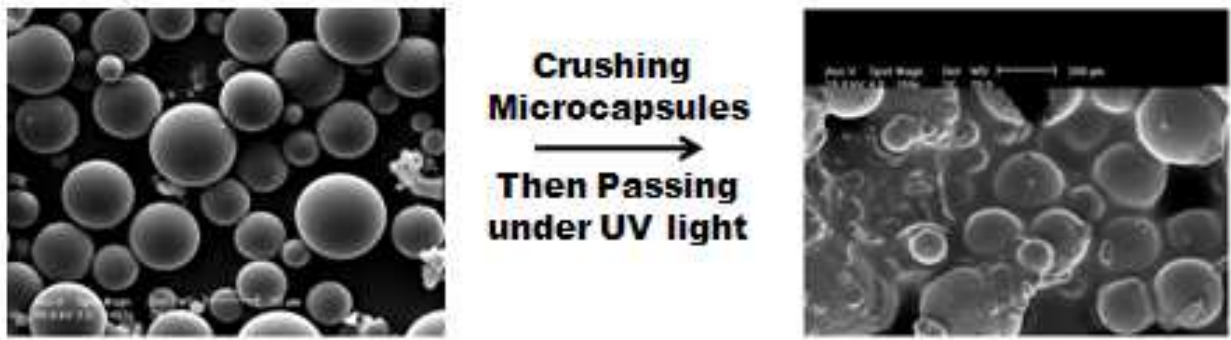


Figure 22. Auto-repairing after cracks

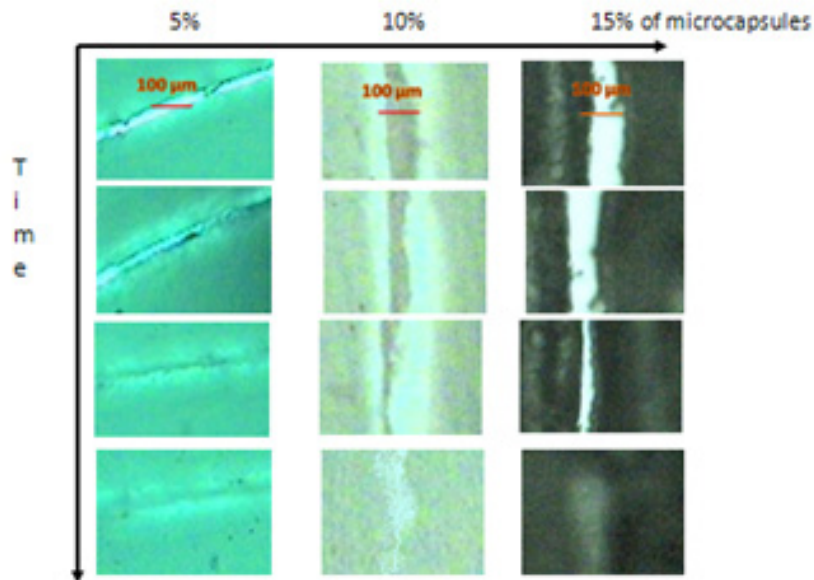


Figure 23. Sel-healing after cracks for 0, 10, 20 and 30 min of irradiation respectively

Simulation of the cosmic effect – Figures 24 (a) and (b), was provided in a simulator SES (Space Environment Simulator) at Yerevan Physics Research Institute at the following conditions (260 nm) – Table 1 below.

Experimental Conditions	Units
Vacuum	1×10^{-5} Torr
Electrons Bombardment	5.0 MeV
Temperature	-50 °C
UV Solar	2.0 kW / sq.m.
Proton Bombardment pfu	> 10 MeV

Table 1. Simulator parameters

PI films loaded with 15 wt. % of Si-microcapsules loaded with TMPTA monomer exposed 30 min are equivalent to 6 month exposure at the real space condition over geostationary orbit of the earth.

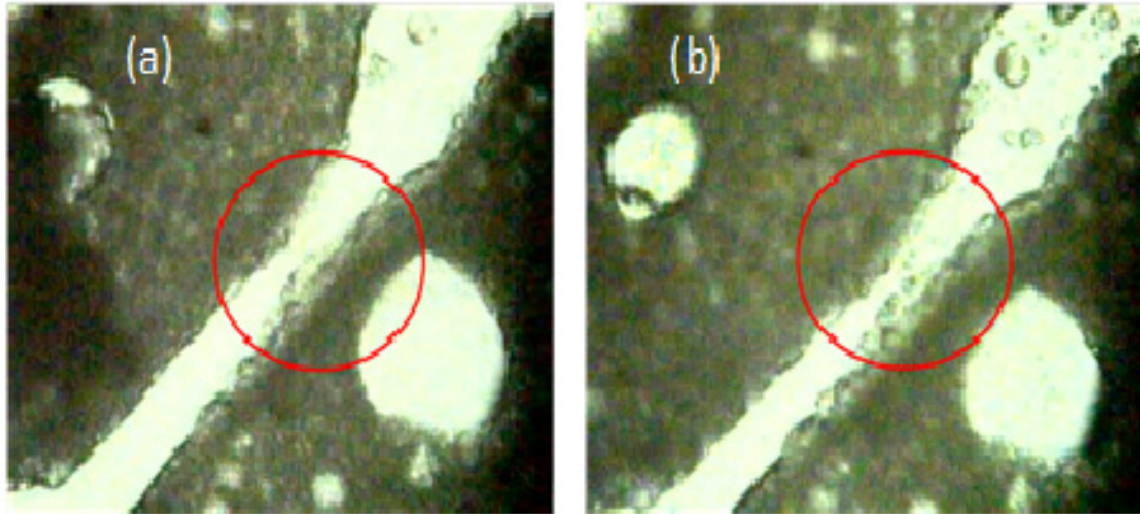


Figure 24. Cracks at time zero (a) – Cracks at exposure time 5 min under 260 nm (b)

5. Mechanical performance of the composite film

The capsules were the defects of the structure in which cracks mainly grew from. The increases in capsules concentration led to a more brittle fracture as shown in Figure 25.

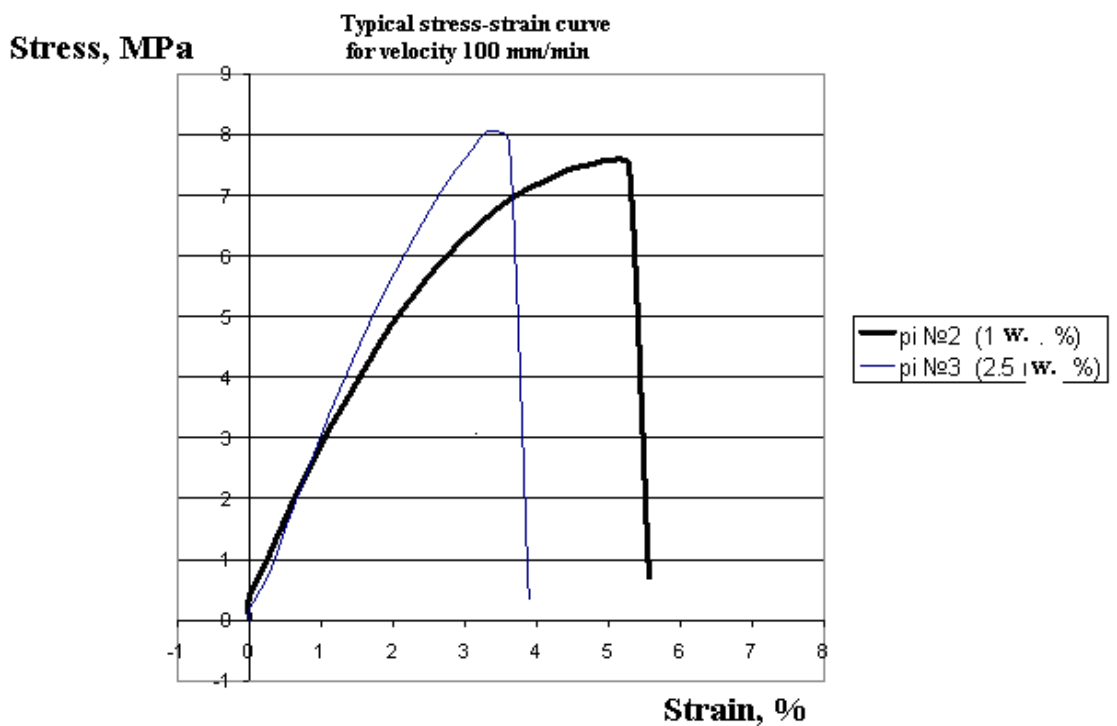


Figure 25. Effect of the wt. % loading on the strain-stress curve

Tensile curves were measured using a universal “Shimadzu” Autograph AGS machine. The test samples were strips with working size of 5x30 mm. The thickness of samples was measured by a magnetic “PosiTector 6000” instrument.

Then, a circular hole (diameter = 0.3 mm) was made in each specimen with the least (0.5 wt. %) and greatest capsules concentration (5 wt. %): Specimens pi-1 and pi-4 respectively. The holes were made by special drill press.

According to the theory of elasticity, the stress concentration coefficient near circular hole is equal to 3 ; in fact the real stress near the hole is approximately one. So, the circular hole might be considered as the standard stress concentrator.

Stress – strain curves for Specimens pi N°1 (0.5 wt. %) and pi N°4 (1.5 wt. %) with hole are represented in Figure 26.

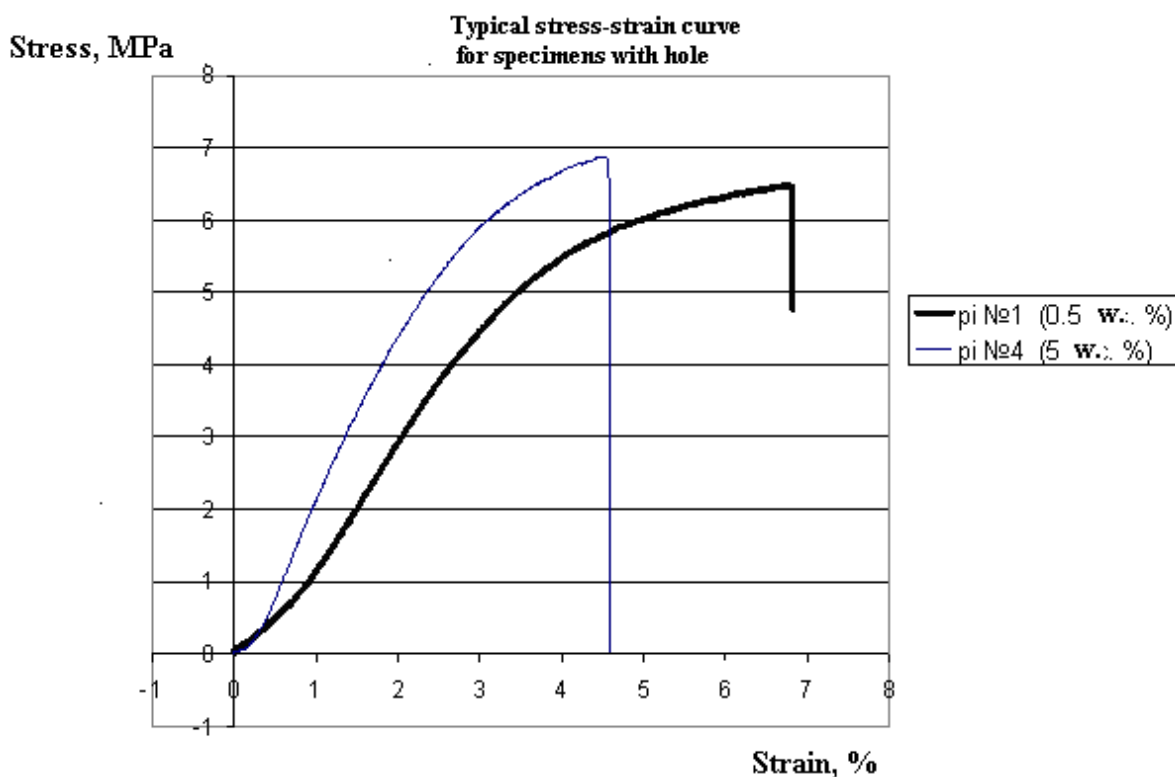


Figure 26. Effect of the wt. % loading on the strain-stress curve of the composite film with hole

The experiment showed that for Specimens pi N°1, the crack passed through the hole. So stress concentration near capsules was less than 3. But for Specimens pi N°4 the crack went through the hole. With the help of this method we can separate films with capsules into two classes: with effective stress concentration less and more than 3.

Using the polarizing microscope POLAR 312, we have detected stress fields near the capsules, even before the loading. It must be taken into account that heat input might be needed for stress relaxation to occur. On Figure 27, stress fields are represented by bright spot.

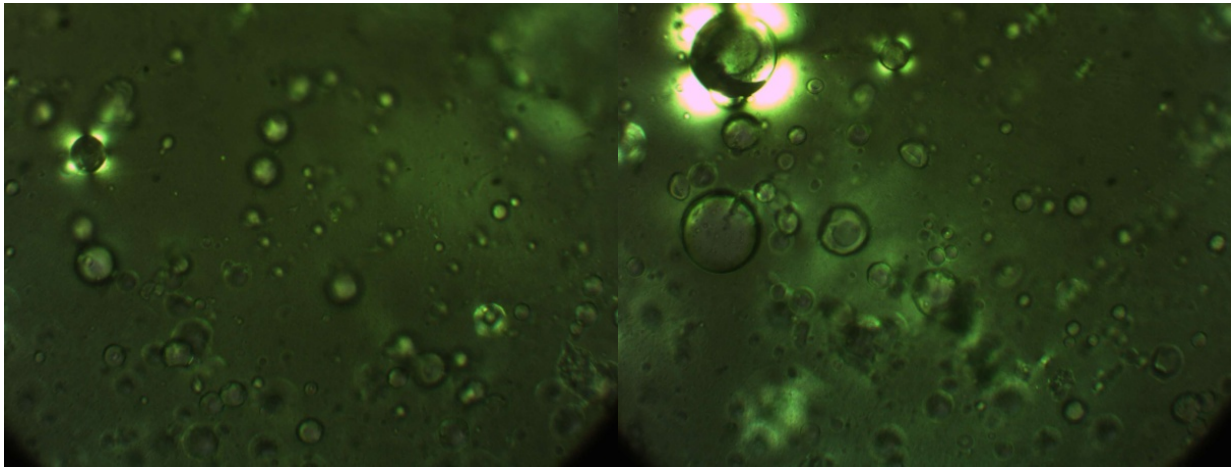


Figure 27. Stress field near hole

Around some capsules, internal strain remained even after rupture of the specimen. In the experiment the film was elongated manually under the microscope by special micromachine.

Stress fields were detected near the hole too as depicted in Figure 28.

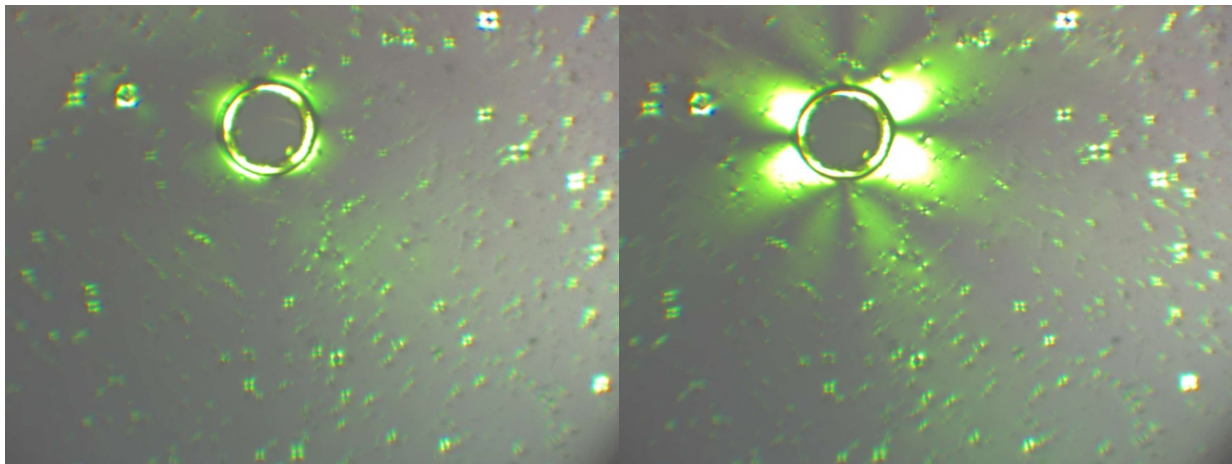


Figure 28. Stress field near hole

The increasing strain near the hole was illustrated in the photos placed in order. The cracks grew through each hole visually. For low concentration of capsules, cracks led to rupture. For high concentration, big crack arose from capsules. It meant that local concentration of stress depended on overlapping of stress fields near capsules too. Theoretically, such interaction appeared when distance between capsules was less than 5 capsule diameters – Figure 29.

These observations allowed us to conclude that stress fields near capsules are the predominant effect; capsules concentration influenced the fracture when stress fields overlapped near capsules.

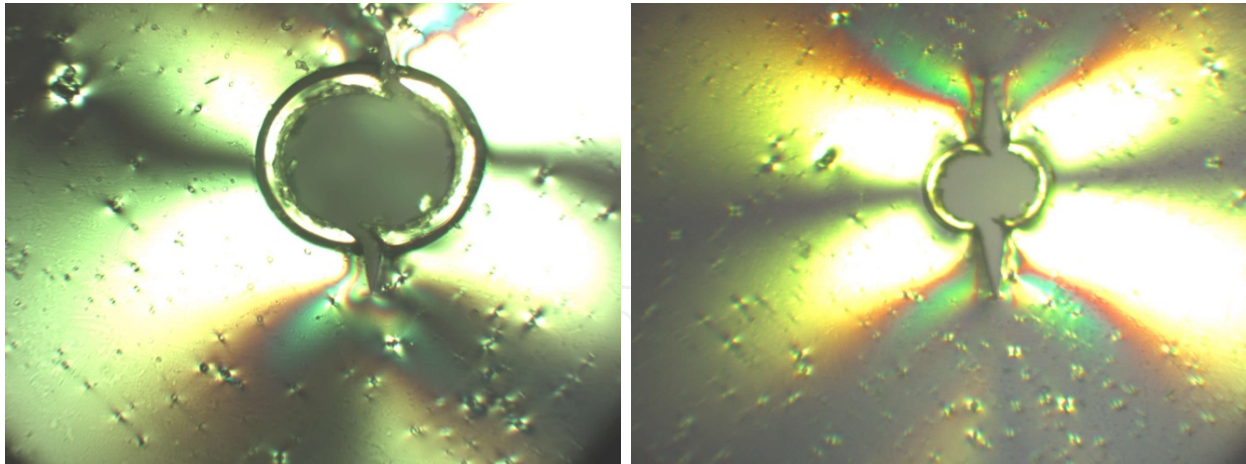


Figure 29. Stress field near hole after elongation

Test pieces were cut from polyimide films. Straight samples, 10 mm in width and 20 mm in length, were tested in tension at 2 mm/min speed with "Shimadzu" "Autograph" machine. The thickness of samples varied from sample to sample and was approximately 0.12 mm. After testing, failed samples were studied under an optical LOMO Mikmed-2 microscope. Hitachi S-520 scanning electronic microscope was used to get a high-magnification image of samples' top and side surfaces, and fracture surfaces of samples were studied with microscopes.

Figure 30 shows the typical stress-strain curves for pure PI film (without particles containing healing resin). The diagram is typical for plastic materials. Initially, the material deformed elastically, and yielding at strain more than 5 % was observed. The Young modulus of fracture deformation of samples was very high, around 130 %.

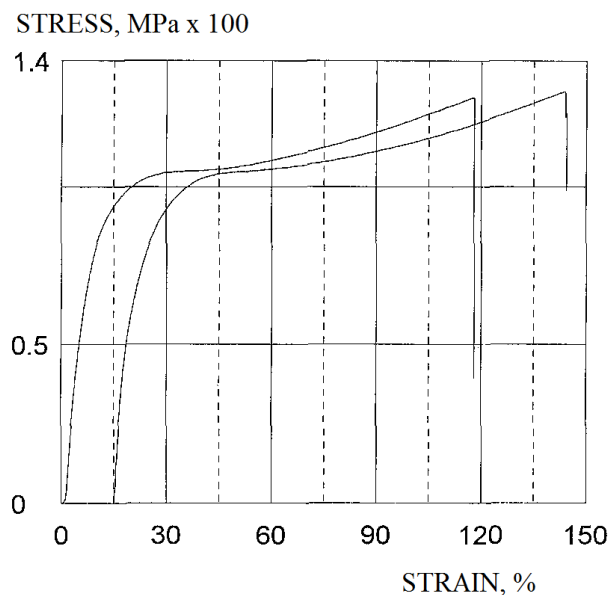


Figure 30. Typical stress-strain curve for pure PI film (without spherical particles)

Figure 31 shows typical stress-strain curves for PI containing 10 wt. % of particles with healing resin. The Young modulus of composite polymer was calculated from the slope of the stress-strain curves to be 2.6 GPa. The curves were similar to that of pure PI. However, the fracture strain was lower at approximately 50 %, due to the stress concentration near particles.

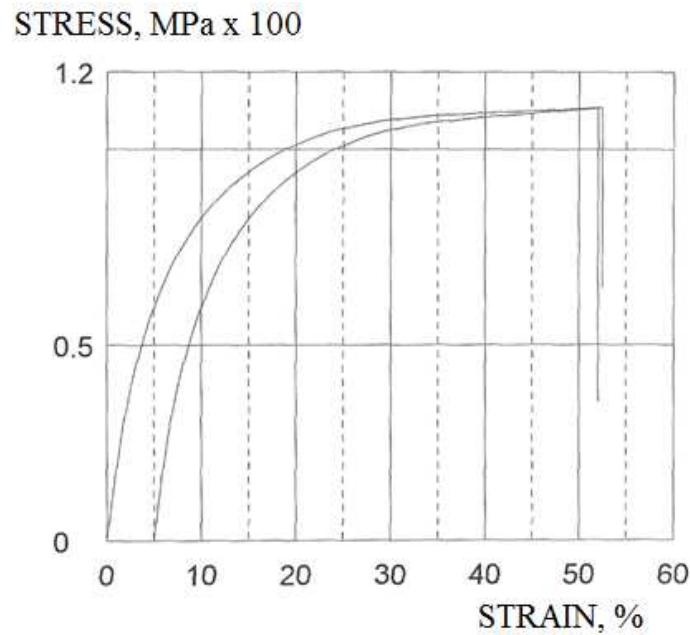


Figure 31. Typical stress-strain curves for PI containing 10 wt. % of spherical particles with healing resin

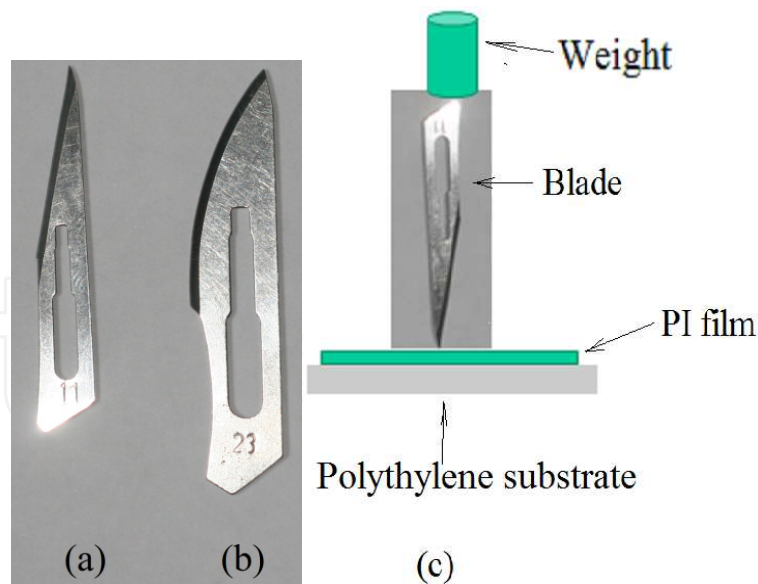


Figure 32. Changeable scalpel blades (a) and (b) used to make a crack in PI film samples. (c) – Method of making through-the-thickness crack

In each sample, two types of cracks were made. First type of cracks was through-the-thickness. These cracks were made by applying 100 g force on a changeable scalpel blade as shown in Figure 32a-c.

The resulting crack is shown in Figure 33 below where spherical particles of different size are observed.

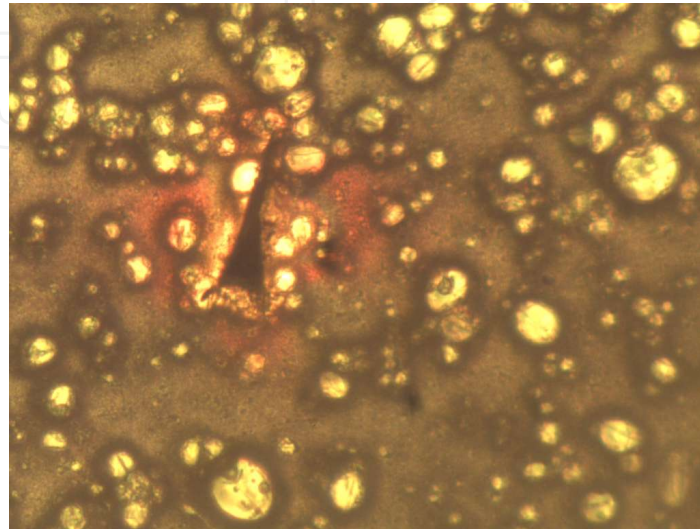


Figure 33. Through-the-thickness triangular crack with the length of approximately 0.6 mm

Figure 34a shows a typical stress-strain curve for composite PI sample with a crack similar to that in Figure 33. The curve is similar to that of composite PI without a crack. The fracture strain was about 18 %, which was typical for ductile materials. However, fracture strain was lower than that in samples without a crack.

Figure 34b shows a stress-strain curve of a similar sample (with a crack) after healing with 200 Watts UV lamp for 30 min. The strength and fracture strain is the same as in Figure 31. Thus, this implied that the healing did not improve mechanical properties if the crack was thick. Possibly, the amount of the liquid resin was not enough to fill the entire volume of the open crack.

The fracture toughness G_{Ic} of filled PI may be estimated from the Figure 31 with the equation below:

$$G_{Ic} = \frac{\pi\sigma^2 c}{E}$$

where σ is fracture stress, c is the half of the crack length and E is the Young modulus of material. Substituting $\sigma = 80$ MPa, $c = 0.6$ mm and $E = 2.6$ GPa, the fracture toughness G_{Ic} is estimated to be 2.6 kJ/m². This value is typical for very tough materials.

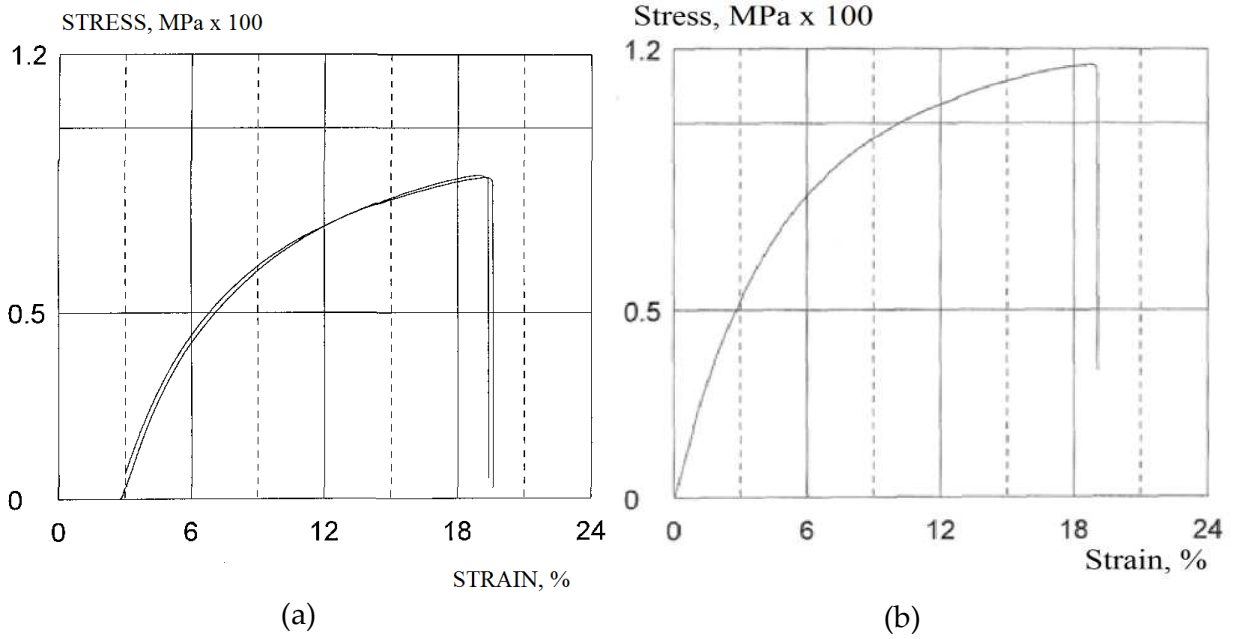


Figure 34. Typical stress-strain curve for filled PI sample with a crack. (a) – without UV irradiation; (b) – after UV irradiation

Different results were obtained from samples with crack of the second type created as shown in Figure 35.

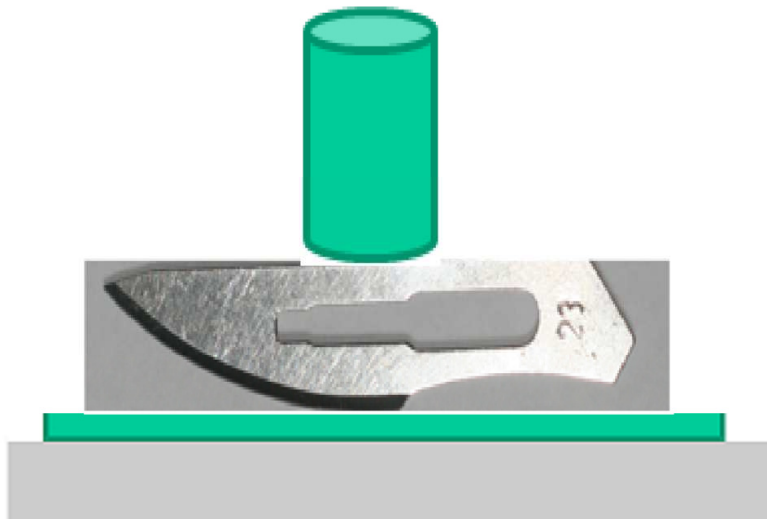


Figure 35. Method of making surface cracks

In this case the crack was on the surface and not deep. These cracks were made by putting 100 g force on a curved scalpel blade. The crack was not wide with low opening, and could not be measured with an optical microscope.

Figure 36 shows typical stress-strain curves for samples with crack subjected to UV irradiation. In this case, two different types stress-strain curves were observed.

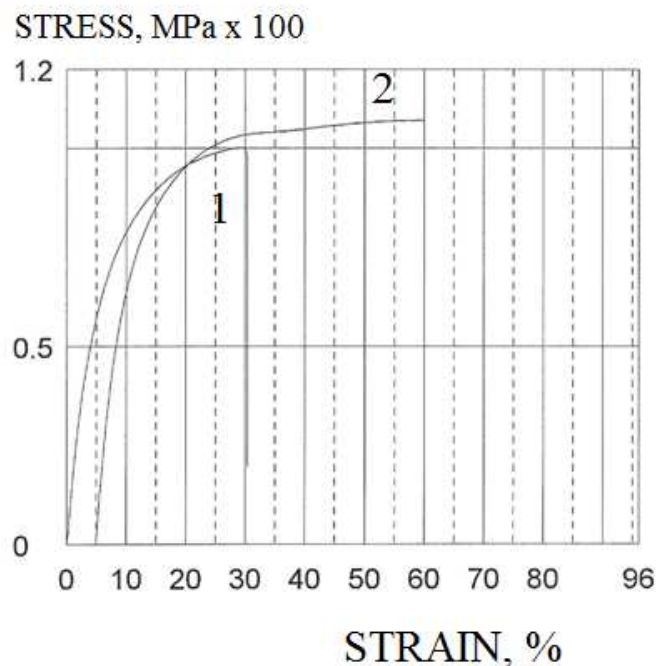


Figure 36. Two types of stress-strain curves for samples with surface cracks made as shown in Figure 35 and irradiated with UV light

The first one is shown by the curve 1 in the Figure 36. In this case the fracture strain is equal to approximately 30 %. This value is higher than that before UV irradiation (20-22 %). The stress-strain curve of the second type is shown by the curve 2 in the Figure 36. In this case the fracture strain is approximately 55 %, which was much higher than in the first case.

In the composite samples two layers were observed: the first one was pure PI and the second was PI filled with spherical particles. Samples with double-layered structure can be observed in Figure 37.

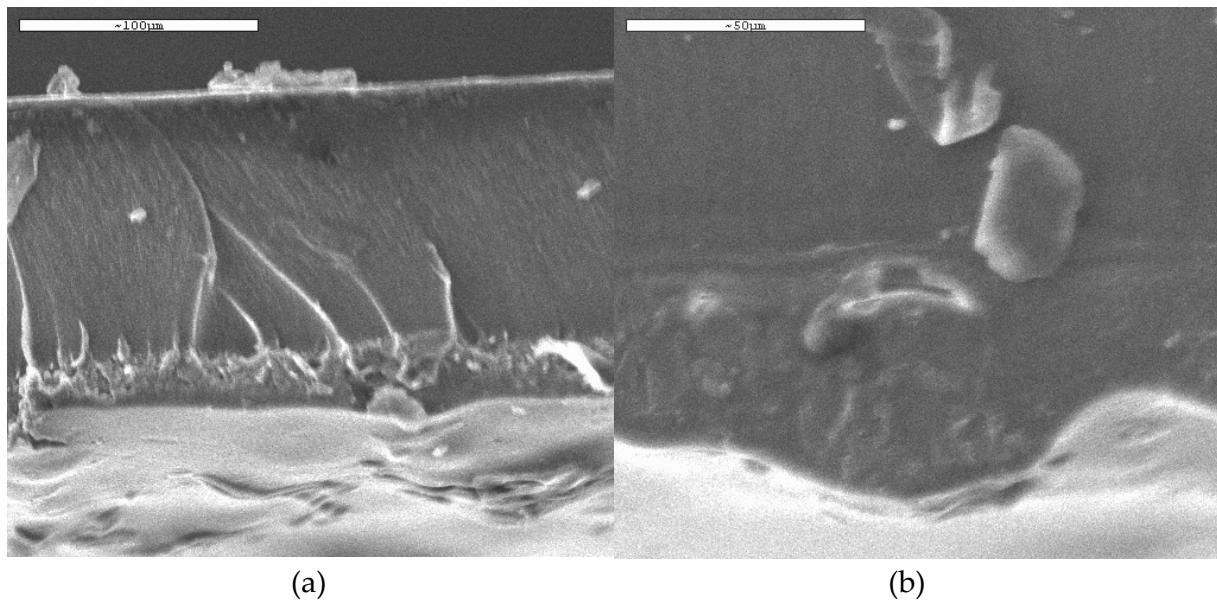


Figure 37. Samples with double-layered structure frozen in liquid nitrogen, at different magnifications. In the right photo, a round particle can be noticed

Study of the fractured samples showed that the layer of the composite PI debonded from the pure PI layer, and this explained higher fracture toughness in this case. Local cracking and debonding of composite surface layer under tensile load can be observed in Figure 38.

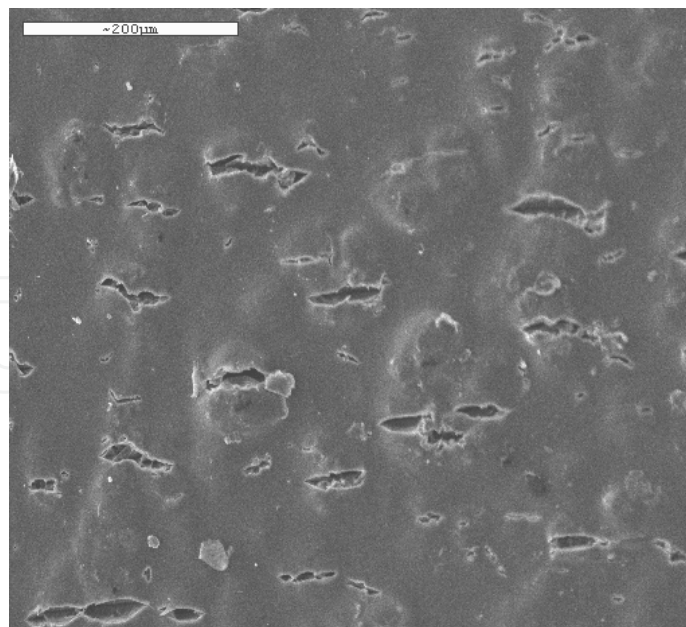


Figure 38. Local cracking of surface layer with PI filled by spherical particles

Schematic drawing of debonding of a surface filled layer near a crack is shown in Figure 39.

Debonding of surface layer with filler particles

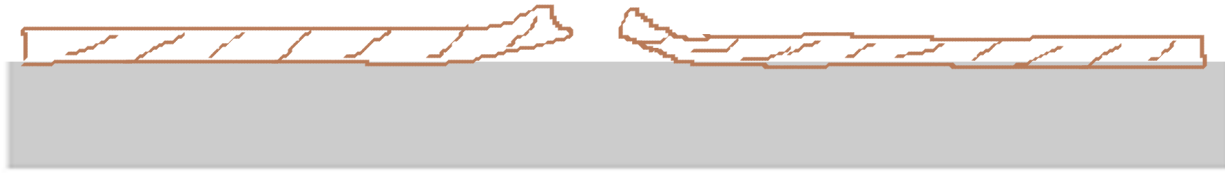


Figure 39. Schematic of debonding of composite layer at the surface near a crack

6. Formulation for low orbital spaceflight

In the condition of low orbital spaceflight (under 30 km), the presence of oxygen might reduce the photospeed of the crosslinking when radical process is used. To overcome this problem we have investigated the use of epoxies initiated by a cationic process of which kinetic is non sensitive to the presence of oxygen [10-13].

For that purpose we have considered a multifunctional epoxy formulations based on dicyclopentadiene and phenolic epoxy, such as solid Epicon-HP720 – Figure 40.

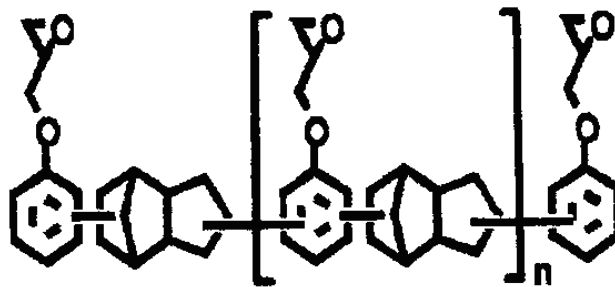


Figure 40. Structure of Epicon-HP720

Different types of co-solvents have been studied in formulating solid epoxy resin (Epicon-HP7200) based either:

1. on epoxy: two cycloaliphatic diepoxy monomers, both having terminal epoxy functional groups at opposite sides of the molecule, being separated by one functional carboxylate, so-called, "space" group in the case of 3,4-epoxycyclohexylmethyl-3,4-epoxycyclohexane carboxylate - Cyracure® UVR-6105 - Figure 41, and by two carboxylate "space" groups in the case of Bis-(3,4-epoxycyclohexyl) adipate - Cyracure® UVR-6128 - Figure 42, and having thus different length of chemical structure have been selected.

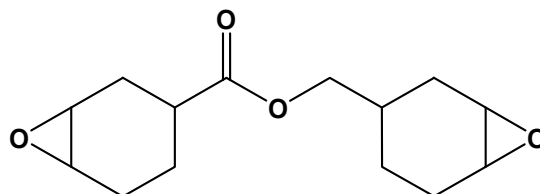


Figure 41.

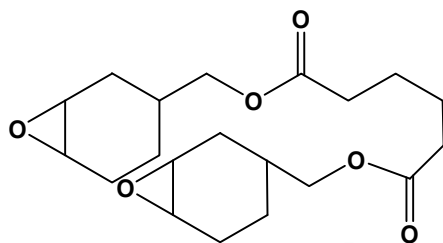


Figure 42.

2. or divinyl ether, triethylene glycoldivinyl ether - Figure 28.

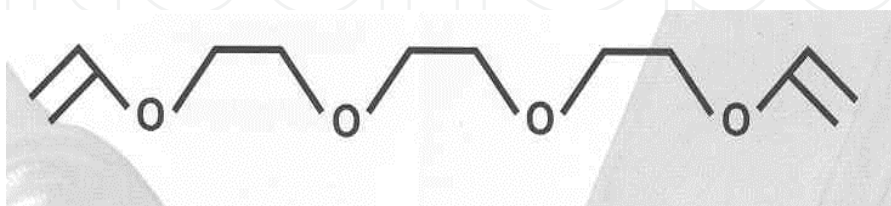


Figure 43. Chemical structure of Triethyleneglycol divinyl ether (Rapid-Cure® DVE-3)

The final objective was to formulate a system based on epoxy having the highest photoreactivity for self-healing applications.

The Photo-Differential Scanning Calorimetry (photo-DSC) [10] was used to study the cure kinetics of UV-initiated photo-polymerization of epoxy resin monomers and vinyl ether in presence of cationic photo-initiator, mainly Cyacure® UVI-6976, former Cyacure® UVI-6974, which consists of a mixture of dihexafluoroantimonate of *S, S', S', S'*-tetraphenylthiobis (4,1-phenylene) disulfonium and hexafluoroantimonate of diphenyl (4-phenylthiophenyl) sulfonium (CAS no. 89452-32-9 and 71449-78-0) at 50 wt. % in propylene carbonate - Figure 44 [11].

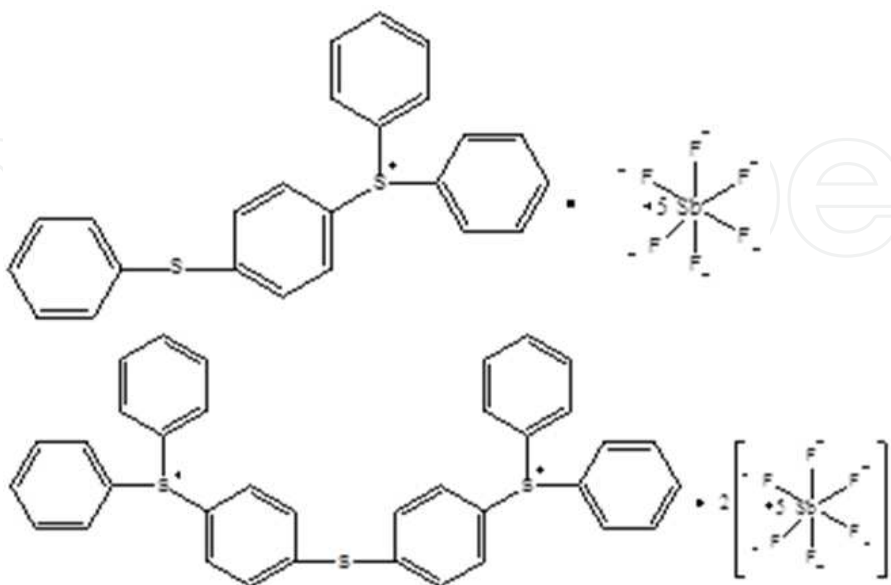


Figure 44. Cationic photoinitiator Cyacure® UVI-6976

We have studied the effect of the temperature for different solvents on the rate coefficient k according to the simplified Sestak and Berggren equation [14] and use the Arrhenius equation to calculate their activation energy E_a – Table 2.

Solvents & Epoxy	E_a (kJ/mol)
Carboxylate (Cyracure® UVR 6105)	7.02 ± 0.80
Adipate (Cyracure® UVR 6128)	4.03 ± 0.20
Vinyl ether (Rapi-Cure® DVE-3)	3.60 ± 0.42
Epiclon HP-7200/Rapi-Cure® DVE-3 (40/60 wt. %)	10.60 ± 0.75

Table 2. Activation energy for different solvents and epoxy Epiclon-HP720 solution

Photocuring kinetic of UV-initiated cationic photo-polymerization of divinyl ether shows a very low activation energy comparing to the two epoxies studied above. The Epiclon HP-7200/ Rapi-Cure DVE-3 system has been optimized by Differential Photo Calorimetry (DPC) in presence of cationic photoinitiator Cyracure® UVI-6976.

We have shown that the mixture of a multi-functional epoxy resin Epiclon HP-7200 and divinyl ether Rapid-Cure® DVE-3 for the ratio Epiclon/DVE (60 wt. % / 40 wt. %), is a valuable candidate for UV encapsulation and for further self-healing test.

7. Conclusions

Silica-organic microcapsules based on 50 wt. % MPTS and 50 wt. % TEOS have been selected to encapsulate the monomer trimethylol propane triacrylate TMPTA and the photoinitiator Darocur® 1173. The microcapsules prepared have diameter size of $4.00 \pm 0.30 \mu\text{m}$ in optimal synthesis conditions: reaction time of 2 h and stirring rate of 450 rpm. These silica-gel macrocapsules have been chosen over urea/formaldehyde or polyurethane due to their thermal stability up to 375 °C.

We have demonstrated the feasibility of self-healing of Polyimide films as coating using a photo-radical mechanism to crosslink the TMPTA monomer.

Mechanical properties of film coatings have been investigated and found that -Stress fields near capsules are the essential factor -Large through-the-thickness and side cracks are not healed -Short surface cracks are healed and Debonding of the surface layer containing spherical particles is the most effective mechanism of healing.

For low orbital spaceflight (under 30 km) where there is the presence of small amount of oxygen, the photoreactivity of different formulations based on epoxies and vinyl ethers have been optimized by DPC, showing the feasibility of self-healing in using a photo-cationic mechanism.

Author details

A.A. Périchaud

Catalyse Ltd., Marseille, France

R.M. Iskakov

Institute of Chemical Sciences, Almaty, Kazakhstan

Kazakh British Technical University, Almaty, Kazakhstan

Andrey Kurbatov and T. Z. Akhmetov

Centre of Physico-Chemical Analyses of al-Farabi Kazakh National University, Almaty, Kazakhstan

O.Y. Prokohdko

Physics Department of al-Farabi Kazakh National University, Almaty, Kazakhstan

Irina V. Razumovskaya and Sergey L. Bazhenov

Solid State Physics Department of Federal Educational Establishment

of Higher Professional Education "Moscow State Pedagogical University", Russia

P.Y. Apel

Joint Institute of Nuclear Researches, Dubna, Moscow, Russia

V. Yu. Voytekunas

Laboratory of Polymer Science & Advanced Organic Materials LEMP/MAO, CC 021,

Université Montpellier II, Sciences et Techniques du Languedoc, Place Eugène Bataillon, France

M.J.M. Abadie

Laboratory of Polymer Science & Advanced Organic Materials LEMP/MAO, CC 021,

Université Montpellier II, Sciences et Techniques du Languedoc, Place Eugène Bataillon, France

School of Materials Science & Engineering, Block N4.1, College of Engineering,

Nanyang Technological University, Singapore

8. References

- [1] M.R. Kessler – *Self-Healing: a New Paradigm in Material Designs*. Proc. IMechE vol. 221, Part G: J. Aerospace Engineering, 479-495 (2007)
- [2] S.R. White, N.R. Sottos, Geubelle, J.S. Moore, M.R. Kessler, S.R. Sriram, E.N. Brown & S. Viswanathan - *Autonomic Healing of Polymer Composites*. Nature, 409, 794-797 (2001)
- [3] S. Cho, H. M. Andersson, S.R. White, N.R. Sottos & P. Braun - *Environmentally Stable Polydimethylsiloxane-Based Self-Healing of Polymers*. Advanced Materials 18 (8) 997-1000 (2006)
- [4] S. Cho, H.M. Andersson, S.R. White, N.R. Sottos & P. Braun - *Environmentally Stable Polydimethylsiloxane-Based Self-Healing of Polymers*. Advanced Materials 18 (8) 997-1000 (2006)
- [5] A.S. Jones, J.D. Rule, J.S. Moore, N.R. Sottos & S.R. White - *Life Extension of Self-Healing Polymers with Rapidly Growing Fatigue Cracks*. Special Issue of Self-Healing Polymers and Composites, J. Royal Society: Interface, 4, 395-403 (2007)

- [6] A.P. Esser-Kahn, S.A. Odom, N.R. Sottos, S.R. White & J.S. Moore – *Triggered Release from Polymer Capsules*. *Macromolecules*, 44, 5539-5553 (2011)
- [7] C. Dry - U.S. patent 2004/00077844, *Multiple Function, Self-Repairing Composites with Special Adhesives*. (06/30/2006)
- [8] A.A. Périchaud & M. Devassine - *Self-Repairing Composition, Self-Repairing Materials, Self-Repairing Methods and Applications*. Patent WO 2009/115671 A1
- [9] R. Iskakov, A. Périchaud, A. Muzdubaeva, L. Caserta, A. Mirsakieva, B. Khudaibergenov, I. Razumovskaya & P. Apel - *Trimethylolpropanetriacrylate Loaded Nanopores Pc Films with Self-Healing*, Potential Proceeding 3rd International Conference on Self-Healing Materials Bath, UK. 27-29 June 2011
- [10] M.J.M. Abadie & V. Yu. Voytekunas - *New Trends in UV Curing*, *Eur.Chem.Tech.Journal*, 6 67-77 (2004)
- [11] M.J.M. Abadie, N.K. Chia & F.Y.C. Boey - *Cure Kinetics for the Ultraviolet Cationic Polymerization of Cycloliphatic and Diglycidyl Ether of Bisphenol-A (DGEBA) Epoxy Systems with Sulfonium Salt Using an Auto Catalytic Model*. *J. Appl. Polym. Sc.* 7, 86-97 (2002)
- [12] L.L. Ionescu-Vasii & M.J.M. Abadie - *Kinetic Model of Photoinduced Polymerisation of Phenyl Glycidyl Ether Monomer*. *Polym. International* 1998; 47, 221-225 (1998)
- [13] A. Lebel, J. Couve & M.J.M. Abadie - *Study of the Photolysis of Sulfonium Salts. Cationic Photoinitiators*. *C.R. Acad. Sci. Paris, Série II*, 1, 201-207 (1998)
- [14] J. Sestak & G. Berggren - *Study of the Kinetics of the Mechanism of Solid-State Reactions at Increasing Temperatures*. *Thermochimica Acta* 1971; 3: 1-11.

IntechOpen